3D Sand Printer

By

M. Yousaf Shahid

Faizan Rashid

Yasir Nazir

School of Mechanical & Manufacturing Engineering

National University of Sciences & Technology

Islamabad, Pakistan

June, 2018

3D Sand Printer

A Final Year Project Report

Presented to

SCHOOL OF MECHANICAL & MANUFACTURING ENGINEERING

Department of Mechanical Engineering

NUST

ISLAMABAD, PAKISTAN

In Partial Fulfillment
of the Requirements for the Degree of
Bachelors of Mechanical Engineering

by

M.Yousaf Shahid
Yasir Nazir
Faizan Rashid

June 2018

EXAMINATION COMMITTEE

We hereby recommend that the final year project report prepared under our supervision by:

M. Yousaf Shahid	NUST201433567
Yasir Nazir	NUST201432559.
Faizan Rashid	NUST201433626.

Titled: "3D Sand Printer" be accepted in partial fulfillment of the requirements for the award of Bachelors in Mechanical Engineering degree.

Supervisor: Dr Hussain Imran (Assistant Professor)

_____

Dated:

Committee Member: Dr Jawad Alsam (Assistant Professor)

_____

Dated:

Committee Member: Dr Rehan Zahid (Assistant Professor)

_____

Dated:

_____ _____

(Head of Department) (Date)

COUNTERSIGNED

Dated: _____ _____

(Dean / Principal)

ABSTRACT

The conventional Sand casting requires storage of pattern so foundries can again pack sand around them to make a new mold when in batch production or the order is placed again. They have to fabricate according to the geometrical desgin, have to keep the fabricated part in inventory. The foundry is actually paying to have them warehoused. It also requires a great skill and a lot of effort and time is wasted for making a pattern and small mistakes results into complete loss of pattern and it has to be made again. 3D printing system for sandcasting will put an end to the need for such storage and fabrication time will be reduced. It fully automates the simultaneous creation of sand molds of the patterns out of sand. The inner geometries, risers and runners etc. are printed simultaneously. This project can be used for printing 3D mold structures with the use of proper feed materials. It can innovate the casting industry of Pakistan by improving the process on a large scale.

PREFACE

This thesis is presented to the NUST School of Mechanical and Manufacturing Engineering (SMME), Islamabad in partial fulfillment of the requirement of the degree BE Mechanical Engineering for the student authors and describes in detail all the efforts that led to completion of their Final Year Project titled “3D Sand Mold Printer”. This thesis elaborates extensively all the stages that this project went through from conception phase all the way to the finalization phase and also sheds some light on the methodology and calculations that were adopted in order to design the machine and the mold. While organizing this thesis, care has been taken to strictly keep it in accordance with the recommended format provided by the SMME. The authors have made a conscious method to use simple and lucid diction and explain the major concepts of sand casting and additive manufacturing to the readers in a simple yet comprehensive manner. Visual aids like pictures, drawings, tables and graphs etc. have been used wherever necessary to add to the overall clarity of the report. Furthermore, design calculations and formulae have also been written. A dedicated portion at the end identifies certain areas in which there is some room for improvement to make this machine even better and more useful. This portion also points out the aspects on which our juniors can work to get better results from this machine.

ACKNOWLEDGEMENTS

We would like to express our deepest appreciation to our Creator and Sustainer, Allah Almighty, The Most Beneficent and The Most Merciful, who provided us the possibility to complete the report and helped and guided us through each and every step of the project. Indeed nothing is possible without His divine decree. Furthermore, we would also like to acknowledge with much appreciation the crucial role of our parents and siblings who lent us their valuable support through all the ups and downs of our life. We are highly indebted to our Project Supervisor Dr Hussain Imran for his guidance and constant supervision as well as for providing necessary information regarding the project and also for his support in completing the project. He has been a source of continuous support and assisted us wherever possible. We would also like to pay special thanks to the entire staff of the Manufacturing Resource Center (MRC) who have been really helpful. We would like to acknowledge the guidance and support of Dr Mushtaq along with Dr Jawad Aslam and Dr Rehan Zahid. Without their precious help, we could not have completed our project on time. Finally, we would like to thank all the individuals who helped in the completion of this project in one way or the other. Special mention goes to Mr Affan Saeed and Mr Moiz Ahmed for their efforts.

ORIGNALITY REPORT

3d sand printer

ORIGINALITY REPORT

4%	2%	2%	2%
SIMILARITY INDEX	INTERNET SOURCES	PUBLICATIONS	STUDENT PAPERS

PRIMARY SOURCES

1	Submitted to Institute of Technology Blanchardstown Student Paper	1%
2	Meet Upadhyay, Tharmalingam Sivarupan, Mohamed El Mansori. "3D printing for rapid sand casting—A review", Journal of Manufacturing Processes, 2017 Publication	<1%
3	Submitted to M S Ramaiah University of Applied Sciences Student Paper	<1%
4	open.uct.ac.za Internet Source	<1%
5	Sachs, E.. "Three-Dimensional Printing: Rapid Tooling and Prototypes Directly from a CAD Model", CIRP Annals - Manufacturing Technology, 1990 Publication	<1%
6	Submitted to University of Pretoria Student Paper	<1%

COPYRIGHT

Table of Contents

LIST OF TABLES

LIST OF FIGURES

ABBREVIATIONS

RP – Rapid Prototyping

AM–Additive Manufacturing

SLM– Selective Laser Melting

SLS– Selective Laser Sintering

FNB – Furan No Bake

NOMENCLATURE

μ	Coefficient of friction
d_m	Mean diameter
ρ	Density
σ	Stress
∂	Deflection
E	Modulus of Elasticity
ε	Damping ratio
G	Shear modulus
J	Second moment of Area
ω	Angular frequency
r	Frequency Ratio
δ	Static deflection
P_0	Atmospheric pressure
R_e	Reynolds number
μ	Dynamic viscosity
F_0	Harmonic Force
x(t)	System response
ω_n	Natural angular frequency
ω_d	Damping frequency

CHAPTER 1: INTRODUCTION

The two most profound requirements which are necessary for industrial productivity and competitiveness are the reduction in the required time of manufacturing said products and the flexible manufacture of said products in small scale quantities. This requires development of comparatively shorter operation cycles and lead time. Rapid Prototyping reduces these variables and allows for development of various manufacturing methods to bring about innovation. Rapid Prototyping are the techniques that employ computer aided design soft wares to construct a part or assembly in short time. The time for fabrication and to develop necessary tooling (e.g. dies) greatly affects the manufacturing process efficiency and productivity. Tooling serves as a gating item for costs related to manufacturing and are a major factor in determining the batch size for any process. Owing to these factors, rapid prototyping by 3d printing helps to eliminate the need of tooling. [1]

Additive Manufacturing (3D Printing) is a printing process that constructs three dimensional parts or assemblies from CAD data without the need for tooling. A layer by layer printing process constructs CAD data into a physical part. The data for each layer is provided from application of a slicing algorithm to the CAD model. 3D printing is a relatively new process.[2]

The 3D printing process has brought innovation to various manufacturing processes. It is considered to be a major force in recent advancements of sustainability development. It has introduced techniques such as stereo-lithography, fused filament fabrication, laser sintering to name a few.[1]

AM has brought major development to the manufacturing process of casting. Casting is a thousands of years old process to manufacture parts, jewelry and sculptures by pouring liquidized metal into a mold of the desired shape and allowed to solidify in the mold. The mold is then removed from the metal part. The process can employ various materials to make the mold e.g. sand or wax. Sand casting is the most sought after casting process.70% percent of all castings are done by employing sand.3D printing has given forth to new options to sand casting in favor of the old manual techniques in which the mold was constructed by workers.

Investment casting is another process for producing metal castings. It gives high surface finish and also widely used.3D printing directly prints the sand molds with cores and runners. This saves the cost of tooling, lead time to manufacture and operation cycles with less manpower required. Fig 1 shows the comparative study of these processes.

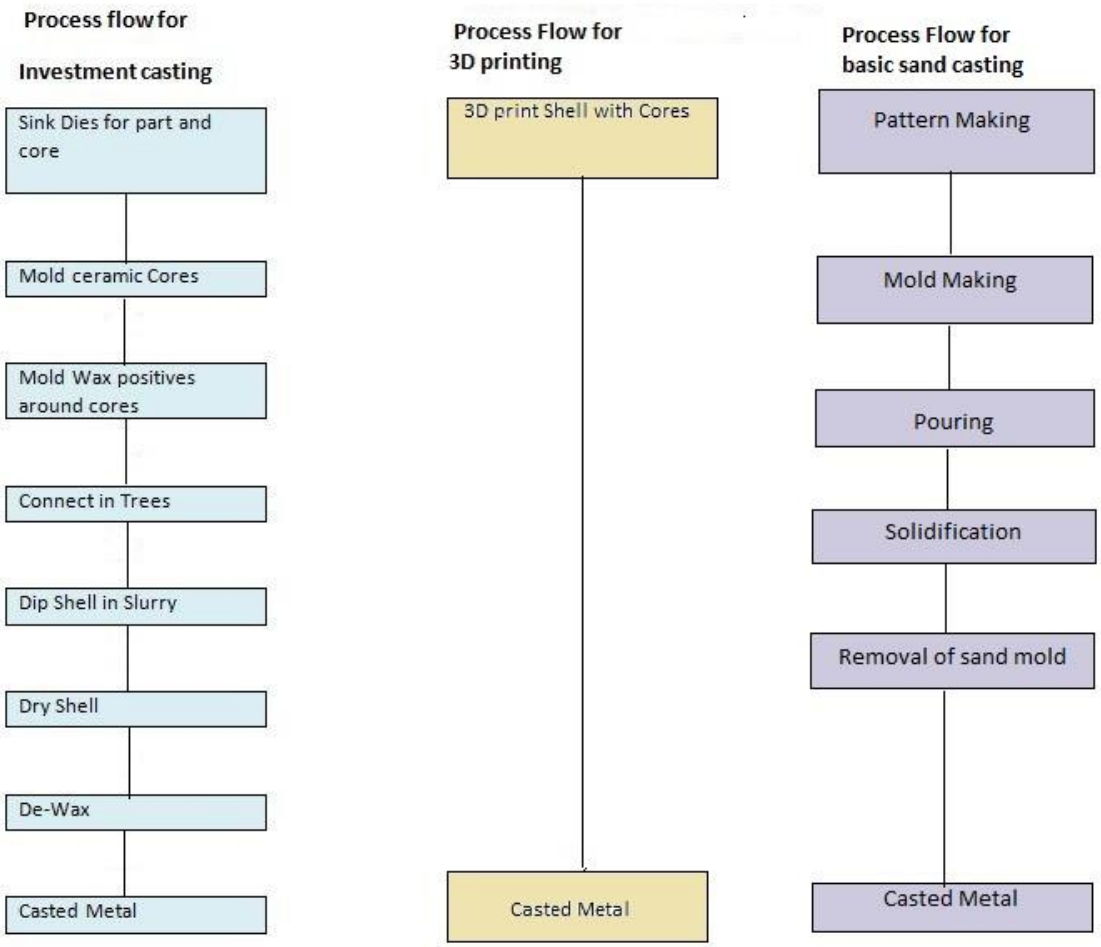

Figure 1: Process Flows

Different types of powders, of varying particle size or shape, and bonding materials can be used to change the thermal and physical properties of the mold and hence give opportunities to explore possibilities for casting a various alloys.3D printing has gained eminence as a cost effective quick casting process that is capable of employing various combinations of materials,

binders and treatment processes to produce complex geometrical patterns that have would relatively be difficult with manual techniques.

The importance of 3D printing to produce complex geometries has substantially increased in the last two decades as casting companies are starting to buy large-scale printers from corporations like Zcorp, ExOne etc.Fig.2 depicts the rising demand for 3D printers for additive manufacturing in the decade since its emergence. Such trends have only increased with added developments.

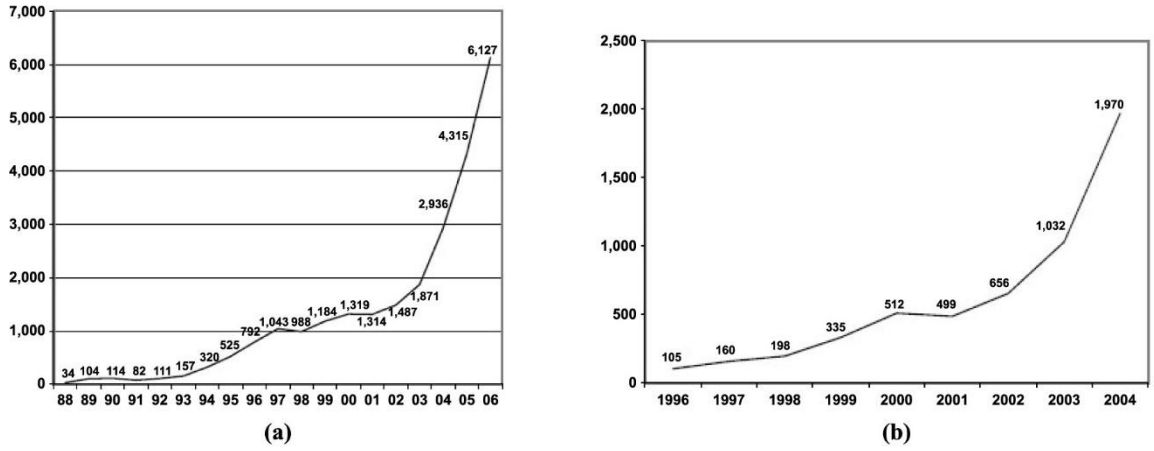

Figure 2: The sale of RP units and 3D printers

The aim of this project is to make a working prototype that provides the benefits of rapid prototyping and using the additive manufacturing process of sand powder bed and binder dispensing to make a mold for casting purposes that in the end can make a solid casting of a part geometry. It is the most cost effective of the various other processes. [3].The ideal end goal is to have a working prototype that can be furthered researched and worked to construct full scale geometrical molds for metal casting purposes whether ferrous or non-ferrous. This will allow a shift in the direction from traditional casting to mechanized casting with the aid of machines.

The scope of this project is limited by the size of mold, batch production and financial support. The current state of casting in Pakistan is not that widespread and the application of 3D printing isn't on the board presently. The project aim is bring in innovation in the casting industry of Pakistan cutting down the cost of tooling (i.e. dies) and various other factors.

The availability and cost of high quality binder and sand is also a limitation in regards to the scope of the project. There is a market demand for process improvement and innovation in this 6000 year old industry especially in the South Asian Belt.

The literature breaks down the researches done on 3DP for casting purposes and the requisite information on binders and actuators.

CHAPTER 2: LITERATURE REVIEW

Rapid Prototyping and Additive Manufacturing

The metal casting industry is widespread and almost 90% of all metallic components are made by casting [4]. In 3D Printing a geometrical CAD model is sliced into layers. For this process a single two dimensional layer is deposited/made in the specified shape of the of the part model. Continuous layer by layer formation in the end results in a 3D part with the initially specified geometry. 3DP is capable of being employed to fabricate various parts of materials like metal, ceramic and polymeric materials. [4].The research and publications in the field of additive manufacturing have been increasing in the last two decades. Figure 3 illustrates the steady increase in the number of publications, it also depicts how this new field still isn't that widespread or advanced.

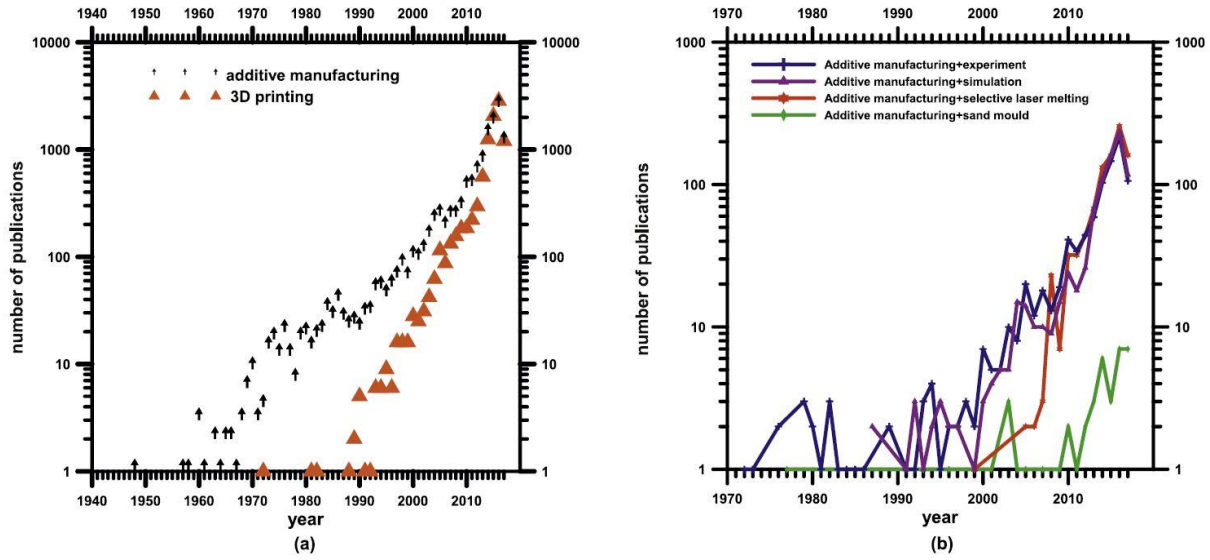

Figure 3: The number of publication in the last decade.[2]

Additive Manufacturing employs 3DP to fabricate parts through layer by layer deposition.[5]There are various additive manufacturing methods that are being used by foundries to construct parts or geometries. One of the most widely known is sterlithography.The process involves photo polymerization [6].The molecules of the powder spread out for each layer are polymerized in the specified shape resulting in the 3d structure. The costs associated is quite

high. Continuous liquid interface production involves the usage of resins and through photo polymerization, the part is constructed.

The additive Manufacturing benefits are stipulated as [7]:

1. AM eliminates the restrictions of the old traditional manufacturing processes and gives room for innovation.
2. It reduces the supply chain and makes the profit space increase.
3. It can reduce the environmental effects as compared to traditional methods.

The most recognizable printing method is the fused deposition method. It employs a continuous stream of fused thermoplastic material. The thermoplastic material is accordingly deposited for each successive layer. The material instantly hardens and takes up the specified shape. [8]

Ultrasonic consolidation is done by the scrubbing of metal foils in the presence of ultrasonic vibrations in a continuous fashion but it is not widely developed for most materials.

Selective laser melting is also an additive manufacturing process that works on the principle of melting and fusing powders through a laser. The process has high surface finish and accuracy. The usage of the laser ensures that the printed part is in high accordance with the CAD model. It began in 1995 at the Fraunhofer Intstitute.It includes a large number of materials like gold, aluminum, titanium and copper in powder form. The costs associated for setup and the fabrication of each part is considerably high.SLM is used in the casting industry to produce sand or ceramic molds for castings that give high porosity and strength. [9].A similar process called selective laser sintering is quite similar in basic concept but differs in the technical properties of the fabricated part. In it, the powder isn't melted but sintered giving rise do differing properties. Due to the exponential costs associated, we therefore did not opt for the SLM process for mold production. Figure 4 illustrates this process.

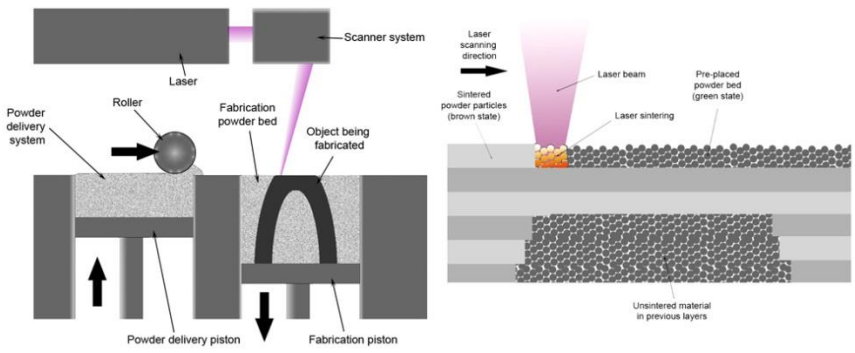

Figure 4: Selective Laser Melting

Powder bed and inkjet Printing employs the usage of inkjet print heads to disperse binder on the powder bed. With each successive layer upon distribution, the inkjet print head disperses binders in the specified zones that upon hardening, a fresh layer of powder is distributed. The particles of the powder stick to each other only in the zones that the binder was dispensed. The remaining un-binded powder still remains loose. Once all the layers are completed, the loose powder is brushed off leaving only the mold. Powder bed and inkjet printing can be integrated for casting purposes by using sand, ceramic or alumina etc. as the powder. It is shown in Fig 5.The binder can be either organic no-bake or inorganic binder that requires heat treatment (baking) after the mold is fabricated. The selection of appropriate binder is discussed in the later section. The Fig.3 shows how research for additive manufacturing for the purpose of casting is very minuscule and developing.

This process is important for smaller scaled production but it can be broadened for large scale production. The advantages that it provides include having the lead time (time for the die to set) reduced, integrating the cores and runners with ease for the mold along with fabricating parts that have highly complex geometries in regards to casting.This process is comparatively cost effective in comparison to selective laser melting

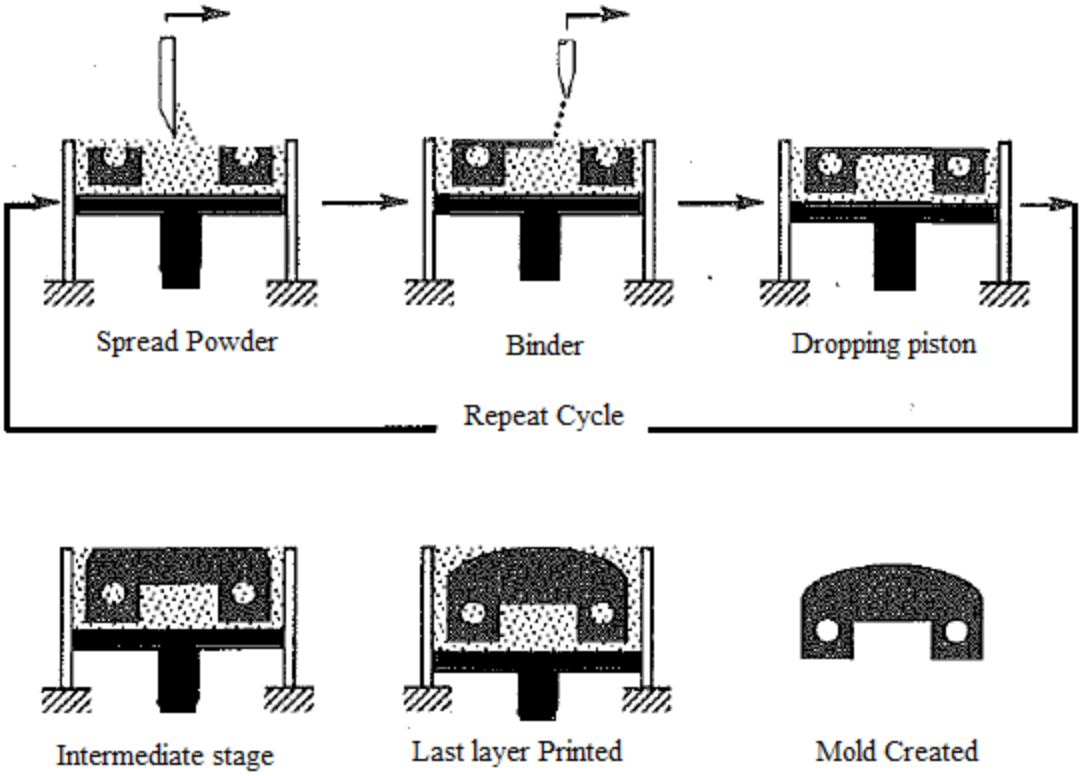

Figure 5: Powder bed and Inkjet printing

Binder and Sand

The characteristics of the sand, the binder type, printing speed and the concentration have a direct effect on the properties of the mold .It has recently been reported that the tensile strength is improved when the layer thickness is decreased and by increasing the binder saturation. This reduces the surface quality as well [10].There has been research done to show that the curing parameters have a direct effect on the mold properties, [11] depicts the relationship between curing temperature with mold properties such as strength and permeability. The binder and powder was provided from ZCast.It was evidenced in ExOne printers that due to well-controlled distribution, the fabricated parts had greater strength (1.3 MPa).

It was reported that even with organic no-bake binders like furan resin or phenolic resin used in traditional casting mechanisms, the 3DP ones performed much better. The 3D printed ones had considerably lower binder content, that gave rise to less gas generation and overall better

castings [12].The correct proportion of binder and catalyst in the case of furan and sulphuric acid provided enhanced strength and resistance [12].ExOne in comparison to other major companies had better performance of its molds in regards to strength , to even distribution of binder on all zones.3D printed sands performed have lower binder content for gas generation in comparison. Table 1 shows the 3DP mold, their binders and properties

Table 1 : 3DP mold, their binders and properties

Ref	Powder	Particle size	Suitable Binder	Properties	Heat Treatment	Application
[13]	Chromite, Silica	140/190/250μm	Furan or Phenol Furan	250-300Ncm^{-2}	None	Casting non-ferrous metals
[14,15] **[13]**	Siilica Zircon Chromite	140/190/250μm	Phenol or Furan Furan	250-300Ncm^{-2}	None	Casting Ferrous metals

The heat that is to be absorbed by the mold upon pouring and the thermal gradient that is present at the interface of the mold and metal has direct impact on the quality of the cast itself. Inverse Fourier Thermal Analysis had been used to determine the binder degradation and thermal properties. The condition was that of casting of aluminum and iron. It was reported that furan had 30% more absorption of heat and a higher rate of absorption. [16].It was reported in [17] that upon a decrease in shell thickness the surface roughness increased. The density and surface

roughness of parts is found to be decreased in certain powder and binder combinations as compared to traditional sand molds.

The 3DP process provides higher flexibility in the printing of the mold with the requisite runners and riser system along with the cores. The studies showed that binder jetting process fabricates parts in shorter times with dimensional tolerances. The volume of production and the geometries complexities have a marked effect on the costs for production [18].

The flow process leaves room for topology optimization in the riser system, runner and cores. Intricate geometries allow for improvement in the placement of these parts. Fig 6 shows the process flow with topology optimization.

Figure 6: Optimization

Binder selection is of utmost importance in regards to the generation mold with high strength and requisite permeability. The binder system depends on which binder is used, which catalyst is mixed with it, if there is an activator in the sand, the comparative proportion of each. There are two major categories of binders, the organic and inorganic. Organic binders don't require heat treatment whereas inorganic do at the end phase. Fig 7 illustrates the difference between them. Furan and Phenol resins are organic binders. Furan binders were made in 1958 to provide for no-bake acid catalyzed systems. The Furan No-Bake System (FNB) system comprises of two parts, the furan resin and an acid catalyst. It can be employed to make all types of castings. The overall quantity of furan binder used is 0.9-1.2% based on sand weight. Catalyst amounts are from 20-

40% based on weight of the binder. The Furan No-Bake system isn't compatible with high demand silica type sands and alkaline aggregates such as olivine.[19]

Like all other no-bake systems, temperature is of paramount importance because the catalyst needs to work in conjunction with the temperature to start and carry out the curing reaction. The color undergoes a change from green to black. Ultraviolet light brings the color back to the original brown.

Furfuryl alcohol is the main basic component in FNB system. They have low Nitrogen contents (from 0-2%).It has 0-30% water content. The higher the grade of furan binder if the nitrogen and water content is low. Furfurly Alcohol is integrated with other chemicals like urea, formaldehyde

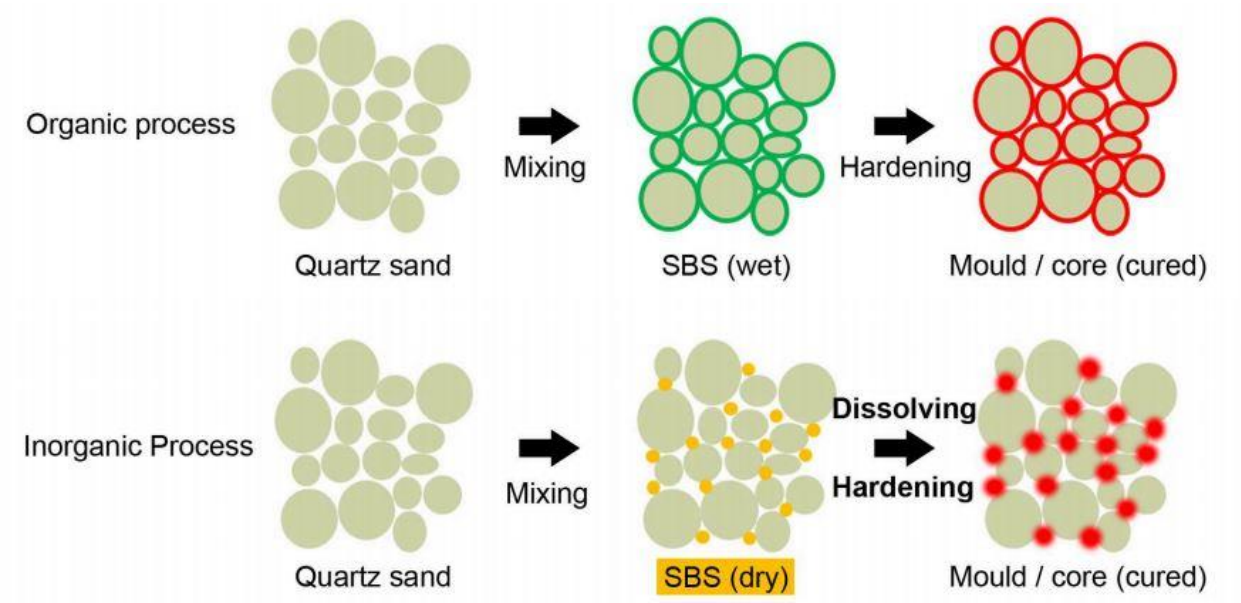

Figure 7: Difference between organic and inorganic binder processes

The main reason for FNB acid catalyzed is to provide neutralization to any alkaline elements in the sand. This helps maintain the curing reaction. Highly concentrated acid is beneficial to the curing rate.

Catalyst choice and potency is essential for binder performance. The speed of the curing reaction is controlled by controlling the quantity of catalyst. Fig 8 Depicts on what factors curing depends on.

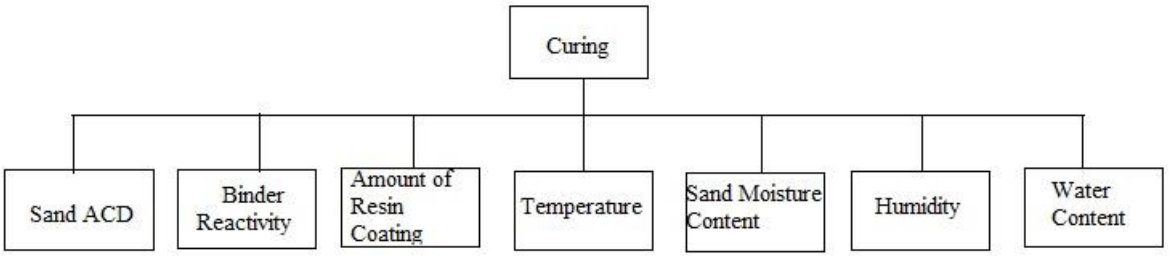

Figure 8: Factors on which curing depend on.

The salt and pepper effect is observed when the acid is added to the dry sand, it fills the spaces between the grains. The end result is that some zones have more acid in them than others. The furan resin meets different packets of grains with varying amounts of acid; it reacts with some zones of sand giving a darker shade upon reaction. The catalyst needs to be added slowly into the sand and mixed thoroughly before the resin is introduced. The resin and catalyst should never be mixed with each other directly. The highly exothermic reaction would result in a explosion. Sand composition is normally in a specified amount in traditional molding as exhibited in table 2, but with advent of FNB system, only dry silica sand is required for 3DP.

Table 2 : Molding Sand Composition

Molding Sand Constituent	Weight %
Silica Sand	92
Clay	8
Water	4

Sand temperature helps to improve the curing reaction. The temperature should be between 70-90 F. The curing rate starts to increase upon the increasing of the temperature and starts to decrease as the temperature starts decreasing within this range. It is preferable to manage the sand temperature than to manage the quantity of catalyst.

FNB systems work best with silica sands. Well cleaned, round silica grains give high quality strength. Lake Sands require high quantities of the acid but beach sand requires an optimal amount. The sand density is increased by compaction before casting process to help in curing. The moisture content needs to be below 0.2% otherwise it slows down the curing reaction.

Furan systems provides a large number of advantages.

1. More reactive binder types can use milder acids like phosphoric
2. Mixing with sand provides good flow ability
3. Lesser smoke and odor
4. It provides recognized polymerization shrinkage.
5. It gives excellent dimensional accuracy
6. Wide variety gives tradeoff between cost and performance.

Phenolic resin is also a non-bake system. The other option besides furan is to use phenol formaldehyde resin with an ester hardener. It has low nitrogen content. It has primarily employed for medium size casting process and is primarily used for core making process.

The general content used for $1.2 - 2.0$ % and the hardener is primarily in $20 - 25\%$.Upon combining with different speed esters in varying quantity to find appropriate curing rates at desired temperatures. The following graphs depict the varying curing rates for high, medium and low speed esters with the temperature tradeoff accordingly. The water content is $14.5\ to\ 15.5$ %.

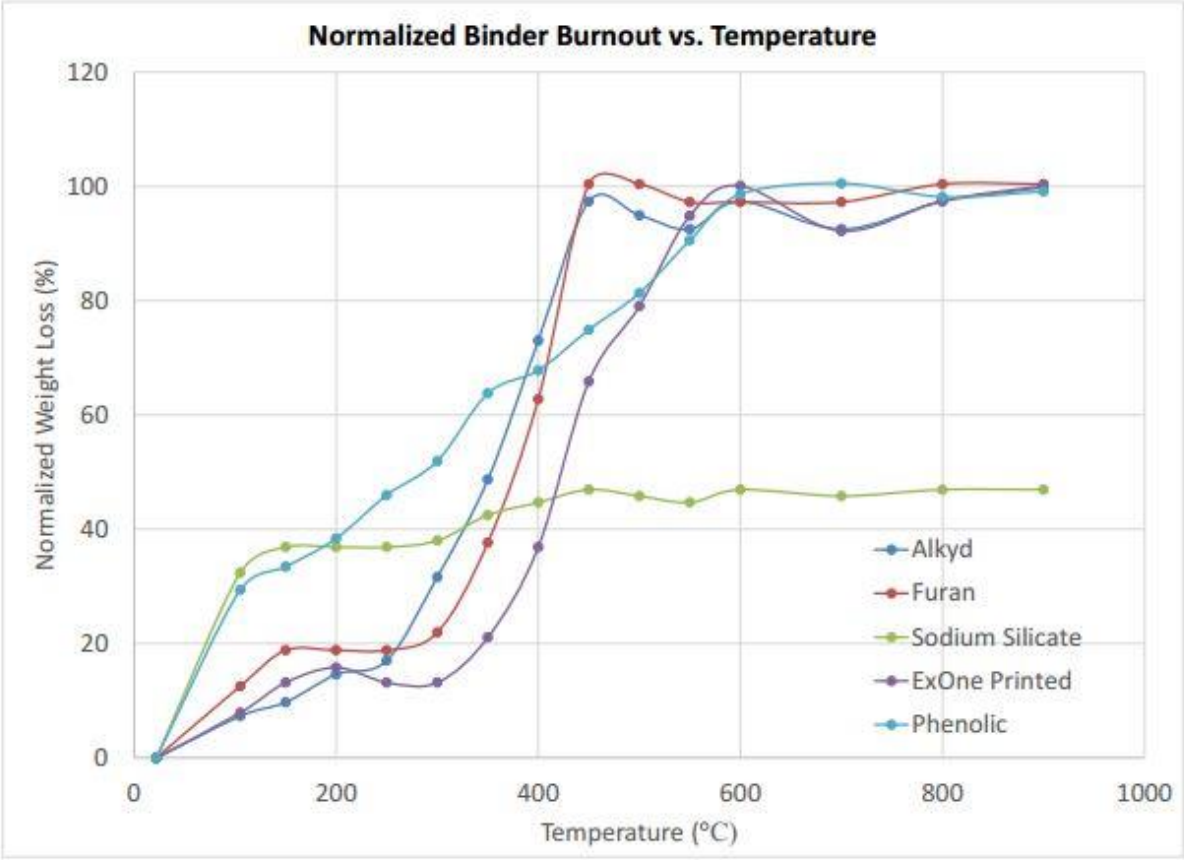

Figure 9: Binder Burnout vs. Temperature [20]

Phenolic Binders are also beneficial because:

1. They don't give out toxic or irritating odors
2. The have excellent shakeout characteristics
3. Its thermoplastic properties reduces mechanical defects
4. They have lower sulfur and nitrogen content
5. The free formaldehyde is 0.1% max
6. It provides flexibility in mold handling

It can be observed from the Fig.9, it can be observed that there are major differences in the binder burnout properties in the 3DP (especially for furan and phenolic) and traditional systems. Beyond 400°C. The burnout has an almost steady value with the normalized weight loss value. For the ExOne FNB system, there is a marked increase in rate of binder burnout at 300 °C. Binder Burnout at lesser temperature is quite suitable for alloys that have lesser melting points. For lower temperature burnouts, there are lesser health and environmental hazards, less cure time and less binder quantity needed. [20]

Keeping in mind the cost of SLM , the powder and Binder jetting process option is the most feasible to undertake and cost effective option to bring innovation to the casting industry of Pakistan. The Project will be initiated at a small scale level with a working prototype and enhanced in the future to work in large scale production as well compete in casting industry market. The one we intend to build will be economical and affordable for smaller startups and companies. It will fabricate parts at a cheaper rate with less tooling and manpower involved. Apart from the initial cost of construction and binder, the remaining charges will be pretty nominal. This includes the electric power for running the printer and miscellaneous costs for operation.

The methodology in the next section deals with how the mathematical analysis that was done on the printer components, it discusses the findings that are necessary to create a working prototype and the overall design.

CHAPTER 3: METHODOLOGY

To achieve the goals and objectives of this project a very simple design for the functioning prototype was made. This model mainly includes two sand beds, one that act as sand feed bed and other as print bed, leveling roller, binder dispensing unit and outer body to hold these in place. Both the sand beds (feed bed and print bed) are individually operated by stepper motor to lift and lower the beds respectively. A leveling roller is used to transfer sand, layer by layer from feed bed to print bed. Binder is dispensed on the sand layer using binder dispensing unit which is a syringe-plunger system, controlled by set of stepper motors to execute movement along x and y axis.

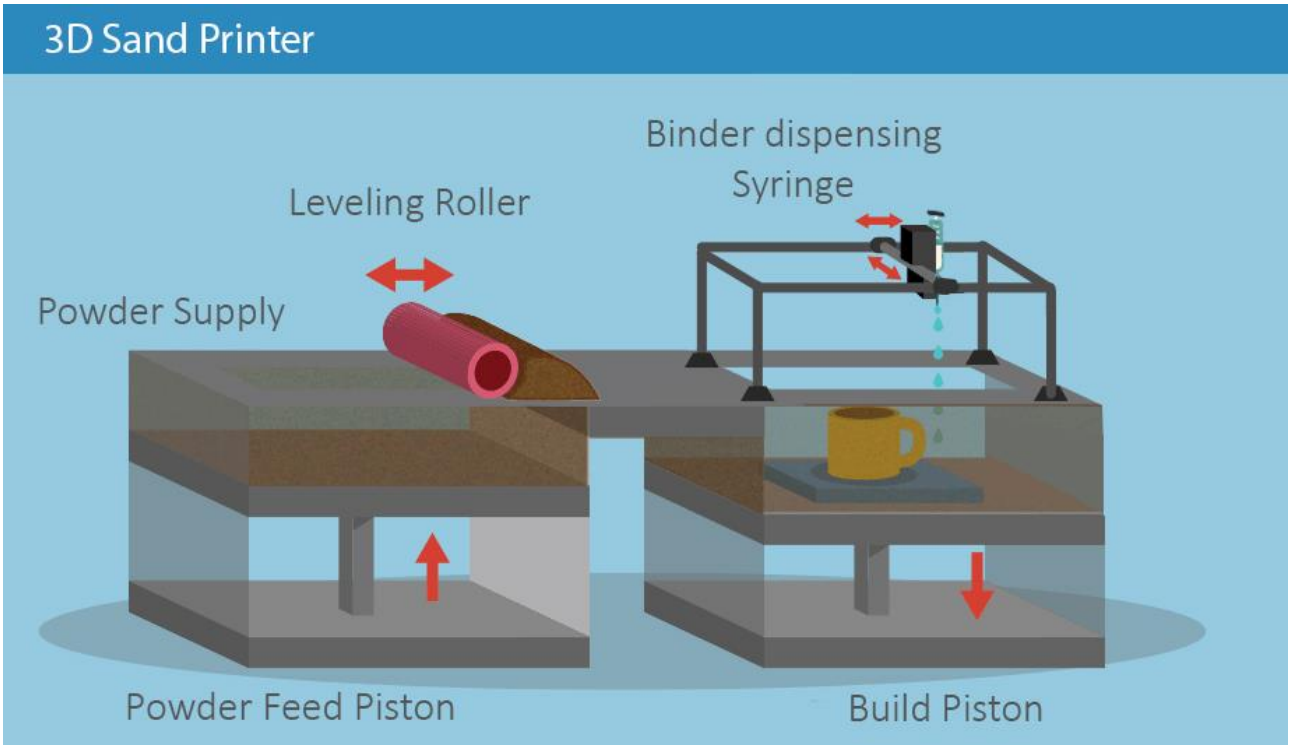

Figure 10: MODEL Drawing

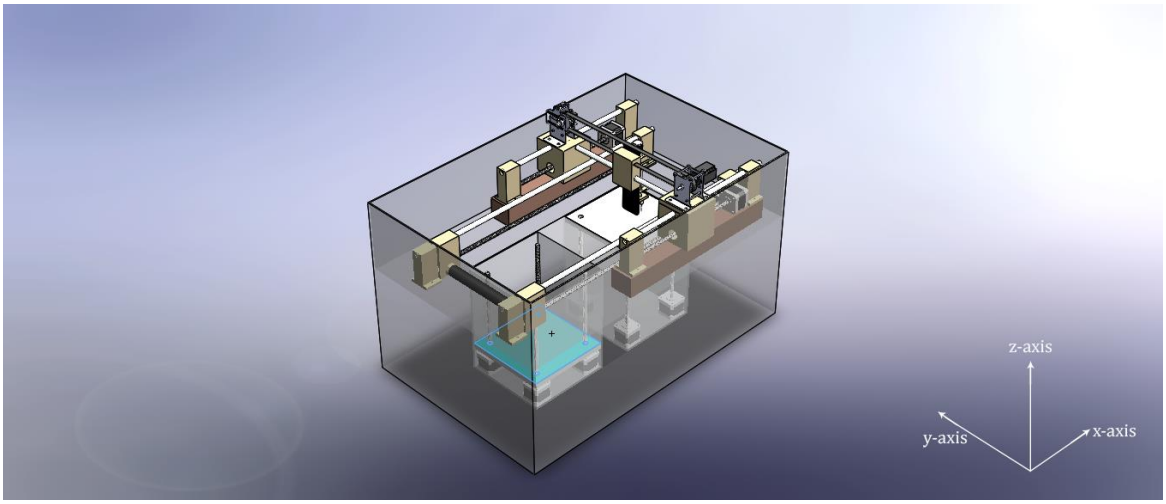

Figure 11: CAD MODEL Isometric View

Each of the bed contains one stepper motor attached to lead screws to enable their movement in z axis.

Movement of levelling roller along x axis is achieved by another of stepper motors and lead screws. Same is the case with binder dispersion unit.

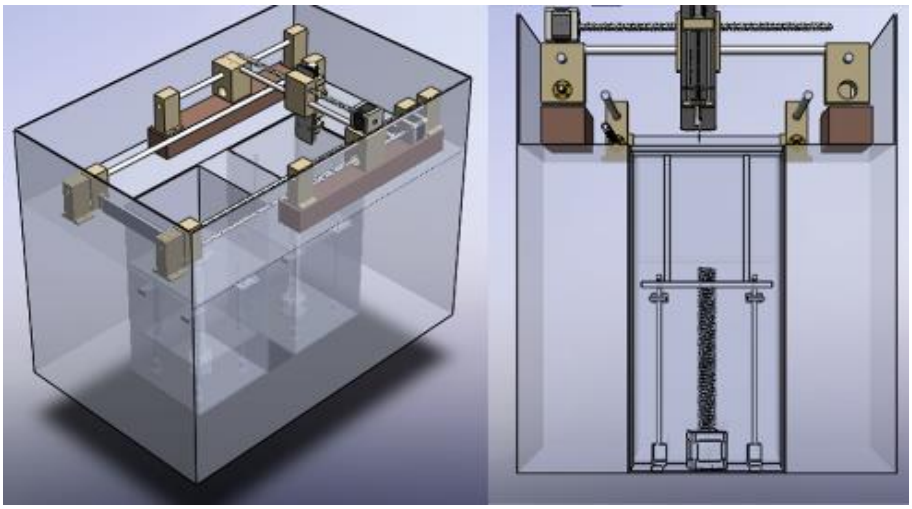

Figure 12:CAD Model Top and Side Views

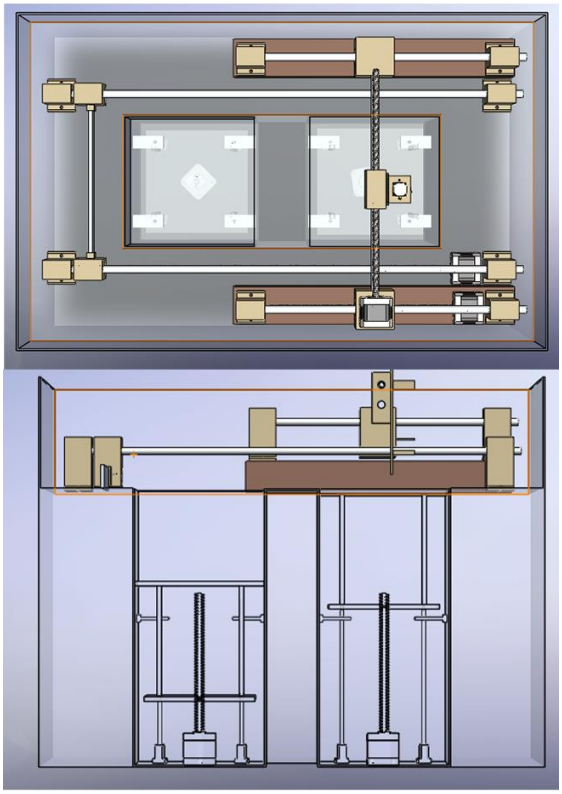

Figure 13: CAD model Front and Side View

Binder is dispersed on the mold bed in the shape generated through 3D CAD model of mold to be prepared. After dispersion, print bed is lowered by lead equal to thickness of sand layer and simultaneously feed bed is raised by the same height. Both these operation are controlled by microcontrollers that control stepper motor operation accordingly. After each bed movement, leveling roller moves from feed bed to print bed transferring next layer of sand over the previous layer which is already been dispensed by binder. Binder then binds both these layer and again dispersion unit is used to displace binder on the new sand layer and the process is repeated till the required height of the mold is achieved. To get better results sand in print bed is constantly maintained at 35^0 C to 45^0 C.

After mold setting time, mold is separated from mold bed and if further heat treatment is not required, is ready to use for casting.

To achieve the said objectives a very systematic approach was adopted. The first step in our approach was work breakdown structure (WBS). Major tasks were sub-divided into smaller tasks.

WORK BREAKDOWN STRUCTURE:

[1] Mathematical Model

1.1 Stepper motor selection

1.1.1 Required lifting torque

1.1.2 Required lowering torque

1.1.3 No. of steps for required lead

1.2 Structural analysis

1.2.1 Compressive stress and buckling of lead screw

1.2.2 Stress and deflection of bed plate

1.2.3 ANSYS analysis of stress and deflection

1.3 Sand bed vibrational analysis

1.3.1 System definition

1.3.2 System response

1.4 Binder jet analysis

1.4.1 System definition

1.4.2 Pressure calculation

1.4.3 Reynolds number calculation

1.5 Transient Respons

- First step in the modeling phase is the selection appropriate stepper motors for the functioning of bed and dispensing unit. For which we have to calculate the torque required and number of micro steps required in achieving the required lead (sand layer thickness).
- Second is the selection of material for overall casing and beds since we have to reduce weight without compromising the strength and material's ability to fulfill the requirement of temperature needed for operation.
- Third step is the vibrational analysis of the beds since the bed may be oscillating at higher amplitude under constant force and overall response of the system to the applied force needs to be taken into account for accuracy of layer thickness. System parts may result into malfunctioning due to higher degree of amplitude or resonance resulting into the overall system failure.
- Pressure required to dispense binder is also needed to be calculated precisely as the flow rate is dependent on the input pressure and flow rate needs to be carefully managed for better binding results.
- Transient response is calculated on the bed to observe stress and strain under constant velocity. It is carried out to check whether the bed remains safe for operation during lifting and lowering

Motor Torque Calculations

Table 3: Torque Consideration Values

Parameter	Notation	Value
Lead screw pitch	P	2 mm
Number of starts	N	4
Lead screw lead	l	8 mm
Length of screw	L	305 mm
Mean diameter	d_m	7 mm
Co-efficient of friction	μ	0.25
Thread angle for square thread	θ	0
Pitch Diameter	d	8mm

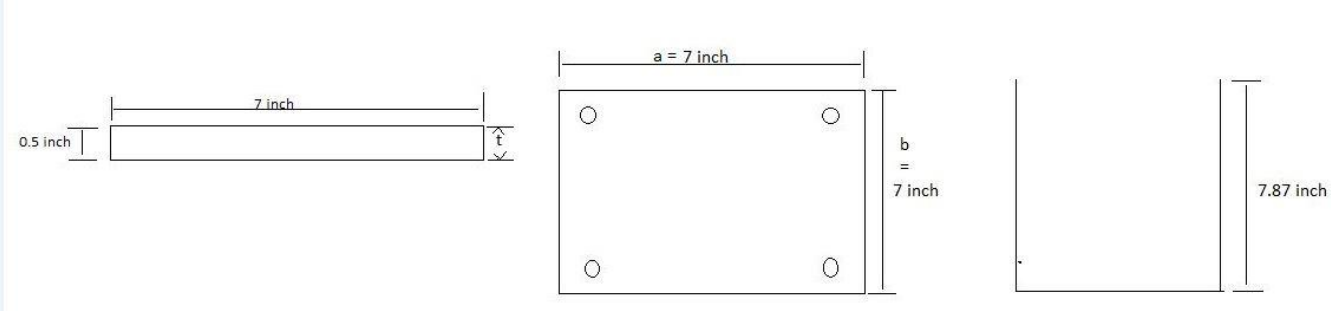

Figure 14: Bed Dimensions

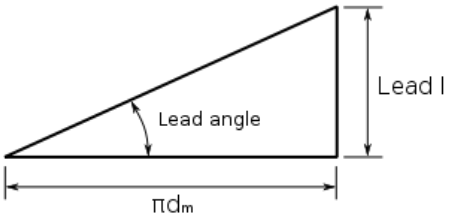

Figure 15: Lead Angle

$$d_m = d - \frac{p}{2} = 7mm \quad d_m = 7mm \qquad Equation\ 1.0$$

$$d_r = d - p = 6mm \qquad Equation\ 1.1$$

For a screw to be self locking coefficient of friction should be greater than tan of lead angle

$\mu > tan\delta$ $Equation$ 1.2

$$Lead\ angle = \frac{lead}{\pi d_m}$$

Lead angle = 0.016 $Equation$ 1.3

→ 0.25 > 0.016

Hence, it will be self-locking.

Volume of container = L x W x H = 0.177 x 0.177 x 0.2 $Equation$ 1.4

= 6.315 x 10^{-3} m^3

Density of sand = ρ = 1120 $\frac{kg}{m^3}$ $Equation$ 1.5

Max mass of sand that can be enclosed = 7 .189 kg

Mass of sand = m = 4kg (Applied on bed for our operation)

Weight force = f = mg= 4 x 9.81 = 39.2 N $Equation$ 1.6

Weight of Aluminum Bed =2700 x {0.1778 x 0.1778 x 0.00635] x 9.81

=5.31 N $Equation$ 1.7

Total Bed Weight = 5.31 + 5.31= 10.63N (for two platforms)

Overall Weight = 10.62 + 39.2= 49.83 N

For lifting

$$T = \frac{\mathrm{F d_m}}{2}\left(\frac{l + \pi\mu \mathrm{d_m}}{\pi d_m - \mu l}\right)$$ $Equation$ 1.8

***T* = 0.1177 Nm**

For lowering

$$T = \frac{\mathrm{F d_m}}{\mathbf{2}}\left(\frac{\pi \mu \mathrm{d_m} - l}{\pi d_m + \mu l}\right) \qquad Equation\ 1.9$$

$$\boldsymbol{T} = \mathbf{-0.0182\ Nm}$$

The required torque for lifting and lowering can be achieved by using **NEMA 17** stepper motor at constant rpm of 400.

Table 4 : Motor Specifications

NEMA 17	
Holding Torque	**0.48 Nm**
Voltage	**12V**
Current	**1.7 Amps**
Phases	**2**
Number of steps / revolution	**200**

This motor provides a micro stepping of 200 in one revolution with each step = 1.8 degrees.

For achieving the required lead of 0.4 mm for sand thickness

Number of Steps = $\frac{200}{8} * 0.4$ =**10 steps**

Motor Control Unit

Components required for motor control unit are listed below:

- Microcontroller
- Motor driver (DRV8825 micro stepping)
- Power supply (220VAC to 12V DC 10A-12A)
- Protection circuit (Electrolytic capacitor 50V 100uF)

Preferably a PCB of protection circuits and drivers

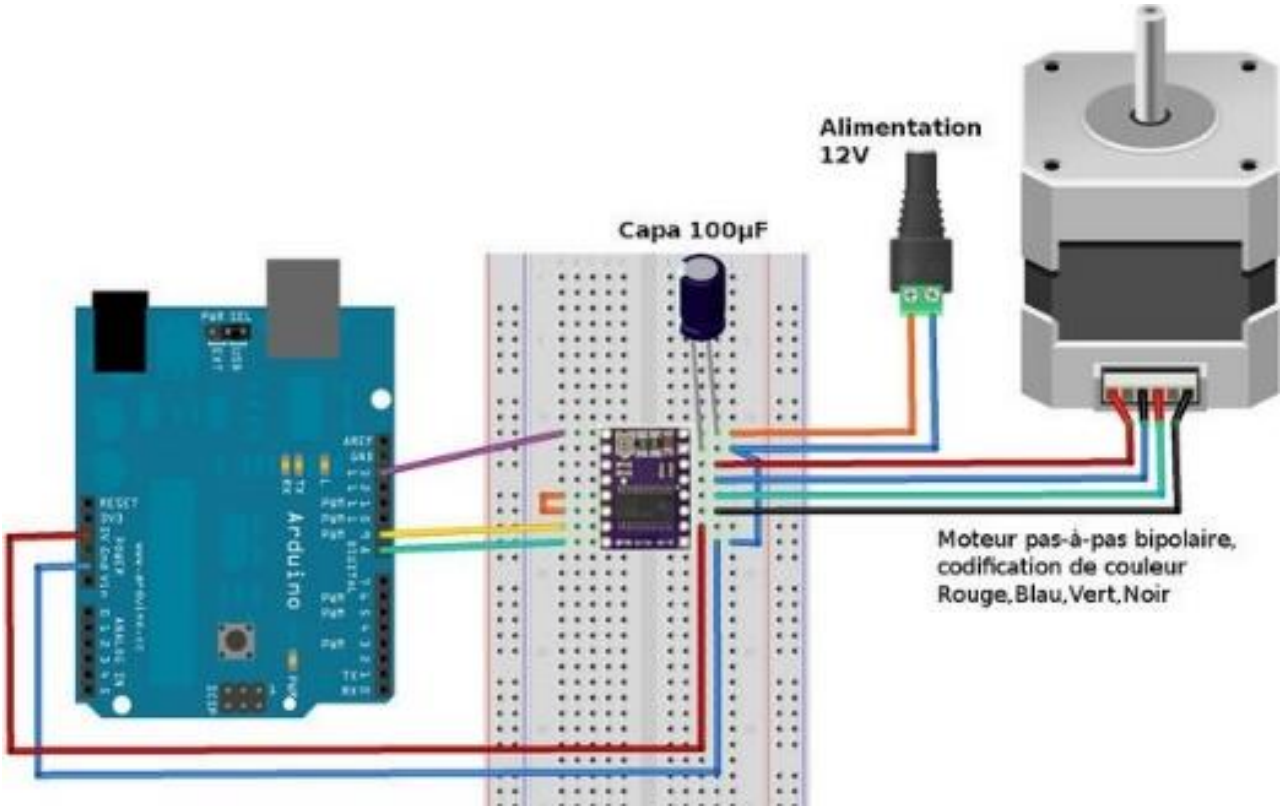

Figure 16: Motor Circuit Alignment

Power Supply

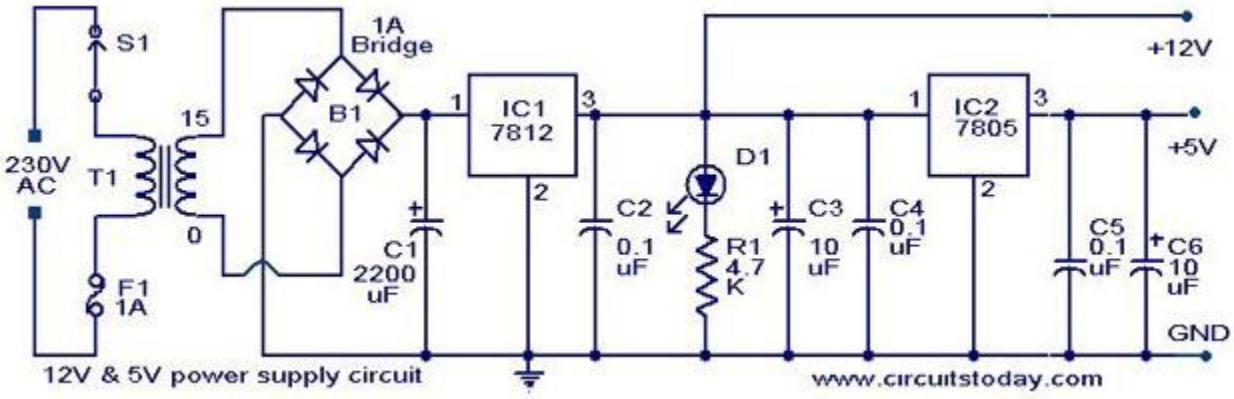

Figure 17: Circuit Diagram

Working of supply

- Step down transformer converts 220V AC to 12V AC
- A bridge rectifier will convert 12V AC to 12V pulsating DC
- Low pass filter (smoothing capacitor) will convert it to 12V DC
- IC 7812 will regulate any fluctuations in the output voltage
- An additional 7805 IC will allow the supply to provide a 5V DC source/output.
- There are additional capacitors for protection from surges.

Micro stepping stepper motor driver circuit

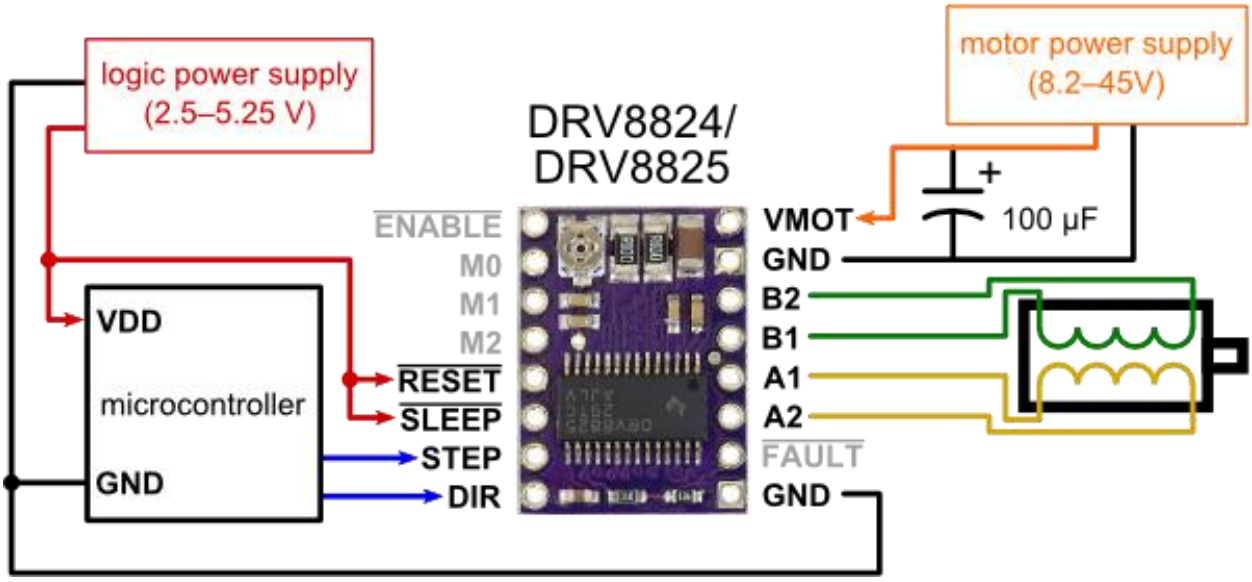

Figure 18: Calibration with DRV8825

Bipolar Stepper motor is connected to pins A1 A2 B1 B2, 12V DC supply is connected to VMOT and GND. For motor to move one-step a digital square pulse is sent to pin STEP and it directions is determined by the digital signal (either 0 or 1) at pin DIR. There are the pins named M0 M1 M2 to determine the mode of micro stepping. DRV8825 can micro step a motor to a factor of ½, ¼, 1/8, 1/16 and 1/32.

Table 5: Motor Modes

MODE0	MODE1	MODE2	Micro step Resolution
LOW	LOW	LOW	Full Step
HIGH	LOW	LOW	Half Step
LOW	HIGH	LOW	1/4 Step
HIGH	HIGH	LOW	1/8 Step
LOW	LOW	HIGH	1/16 Step
HIGH	LOW	HIGH	1/32 Step
LOW	HIGH	HIGH	1/32 Step
HIGH	HIGH	HIGH	1/32 Step

Least count for linear movement of each motor is obtained by driving the motor at the micro stepping resolution of factor 1/32

Angle in one step= $\frac{1.8}{32} = 0.05625^0$

Number of steps in complete revolution= $\frac{360}{0.05625} = 6400\ steps$

Least count of linear movement of motors:

Lead of screw= 8mm

Resolution=$\frac{8}{6400} = 0.00125\ mm$

Resolution for dispersion=$\frac{1}{6400} = 0.000156\ mm$

Component	Pitch of screw mm	Lead mm	Least count mm
Bed screw (z-axis)	2	8	0.00125
Binder dispersion unit (x,y axis)	1	1	0.000156

Stress Calculations for Screw

Compressive Stress:

Compressive stress for a lead screw is given by: $Equation$ 2.0

$$\sigma = -\frac{4F}{\pi(d_r)^2}$$

$$\sigma = \frac{-4 \text{ x } 49.83}{3.14 \text{ x } \left(\frac{6}{100}\right)^2} = -1.7632MPa$$

$$\boldsymbol{\sigma = 1.7632MPa}$$

Torsional Stress:

Torsional stress for the lead screw is calculated as: $Equation$ 2.1

$$\tau = \frac{16T_R}{\pi(d_r)^3}$$

$$\tau = \frac{16\ x\ 0.1177}{3.14\ x\ (0.006)^3}$$

$$\boldsymbol{\tau = 2.77MPa}$$

Buckling

$$P = \frac{n\,\pi^2 EI}{L}$$

$$= \frac{0.25 \text{ x } (3.14)^2 \text{x } 200 \text{ x } 10^9}{0.3048} \text{ x } \frac{\pi(d_r)^4}{64}$$

$$\boldsymbol{P = 337.40\ N}$$

Since our load is 50 N, the design is within safe limits

Stress and deflection of sand BED

Theoretical analysis:

For a flat plate of uniform thickness under uniformly distributed load Stress and deflection are given by[27]:

$$\sigma = \frac{0.75 \text{x} P \text{x} b^2}{t^2[1.61\left(\frac{b}{a}\right)^3 + 1]} \qquad Equation\ 2.2$$

$$\partial = \frac{0.142 \text{x} P \text{x} b^4}{\text{Et}^3[2.21\left(\frac{\text{b}}{\text{a}}\right)^3 + 1]} \qquad Equation\ 2.3$$

Where a corresponds to length of plate and b corresponds to width of plate

In our case a = b (square plate bed), t represents the thickness of plate (Figure: 14)

P=Pressure = $\frac{70.53}{0.1778 \text{ x } 0.1778}$= **2231 Pa** (for max load of 70.53) $Equation\ 2.4$

With three materials under consideration above equations are used to calculate stress and deflection

Table 6: Stress and deflection

Property	Aluminum	Stainless steel	Cast iron
Modulus of elasticity	69 GPa	200 GPa	169 GPa
stress	1.2477 Pa	1.2477 Pa	1.2477 Pa
Deflection	6.925 x $10^{-7}m$	2.389 x 10^{-7}m	2.827 x10^{-7} m

ANSYS Analysis

Following figures the ANSYS definition of the bed plate that includes defining fixed support, creating Mesh of the plate and final definition of pressure distribution.

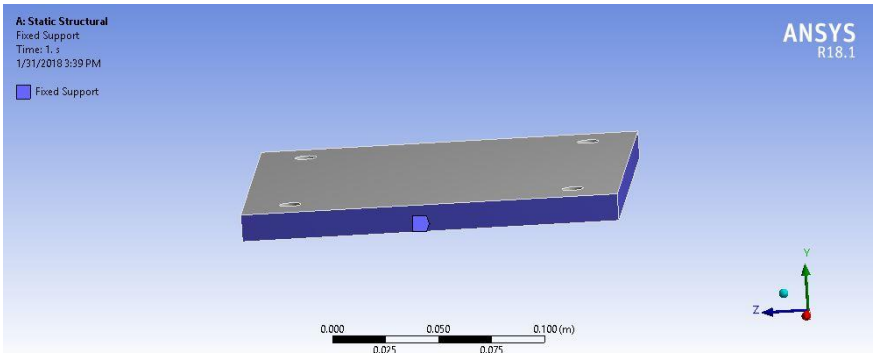

Figure 19: Fixed support

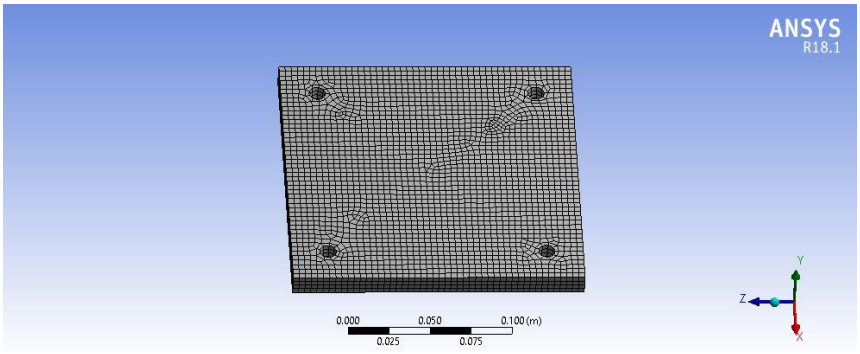

Figure 20: Mesh of Powder Bed Model

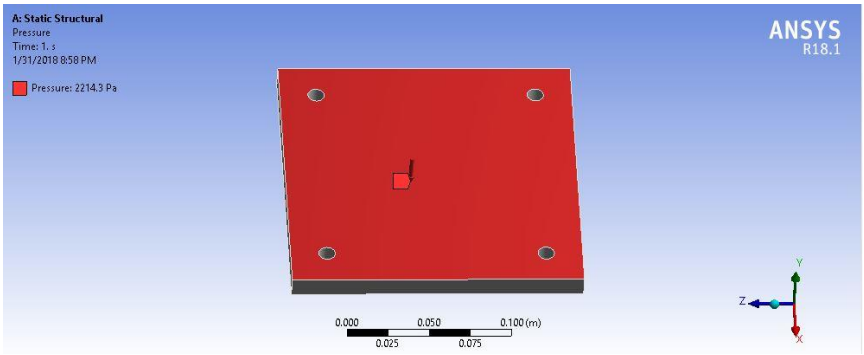

Figure 21: Pressure Distribution

Aluminum:

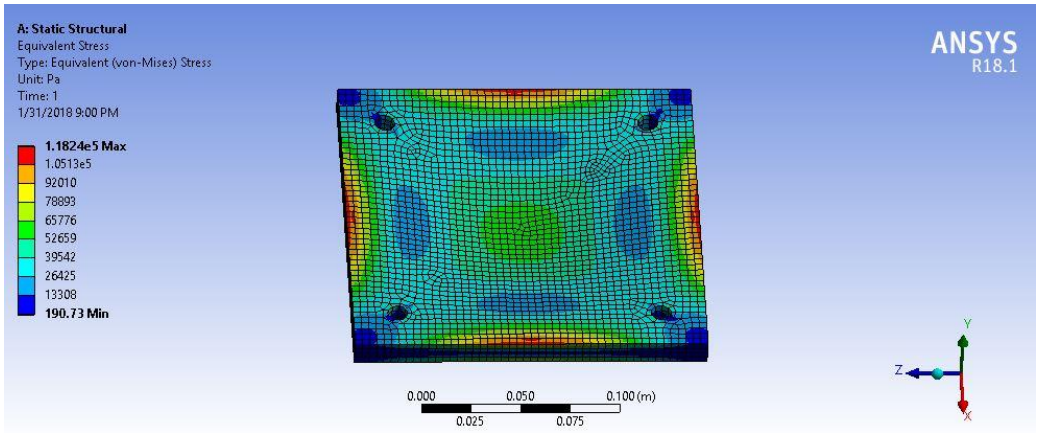

Figure 22: Aluminum Stress

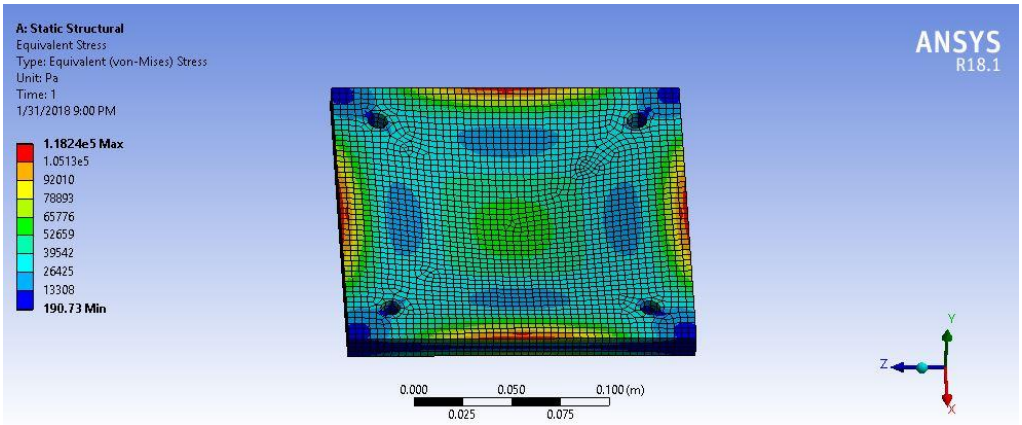

Figure 23 : Aluminum Strain

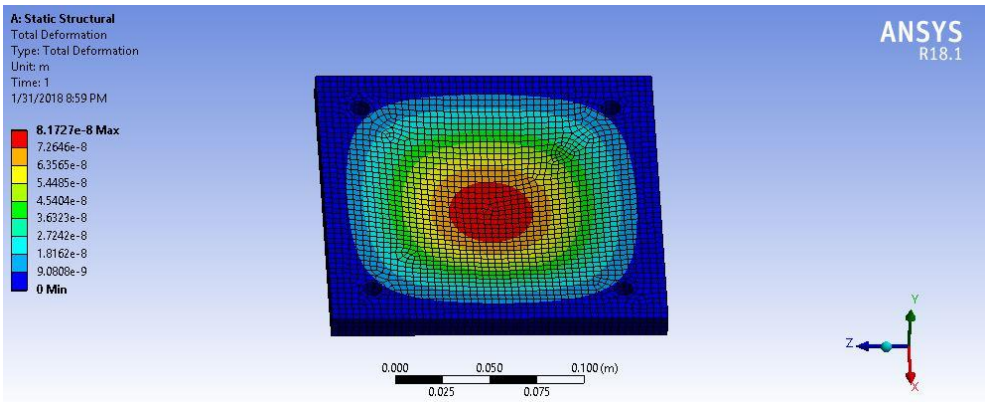

Figure 24: Aluminum Deformation

Vibration Analysis

Table 7 : Platform Values

Parameter	Notation	Value
Mass platform (max)	M	7.07 kg
Mass of screw	m	0.48356 kg
Damping ratio	ε	0.002
Motor Speed	N	1000 rpm
Motor Torque	T	0.48 N-m
Radius	r	0.01 m
Shear modulus (steel)	G	77.2 Gpa
Initial displacement	x_0	0
Initial velocity	$\dot{x}_0$	0

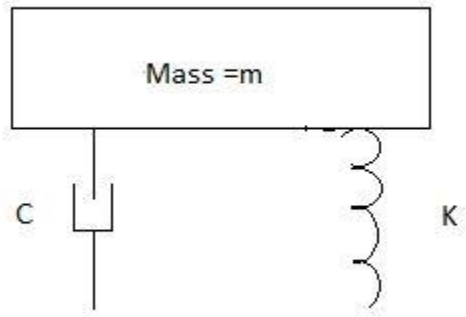

Figure 25 : Vibrational system Diagram of Platform

For the geometry of lead screw, a circular solid rod spring constant / stiffness is calculated from the general twisting equation as: *Equation* 3.0 *and Equation* 3.1

$$\frac{T}{J} = \frac{G\theta}{l}$$

K=T/θ $\rightarrow$

$$K = \frac{GJ}{l}$$

$$J = \frac{\pi {d_m}^4}{32}$$

Given system experiences constant force that is provided by the motor's rotor to the lead screw. Since the torque of motor is the function of its rpm that means the force associated with it is also harmonic and is the function of angular frequency of motor. Magnitude of this force is calculated from motor torque as

$\tau = r_0 \text{x } F$ $Equation$ 3.2

Where r_0 is the radius of lead screw attached to motor's rotor.

Since given force is harmonic, overall force is given by:

$F(t) = F_o \cos(\omega t)$ $Equation$ 3.3

Where ω is the angular frequency of motor providing harmonic force. From motor Speed (rpm):

For max speed at 1000 rpm

$$\omega = \frac{2N\pi}{60} \quad Equation\ 3.4$$

$$J_0 = ml^2 \quad Equation\ 3.5$$

$$\omega_n = \sqrt{\frac{K}{J_0}} \quad Equation\ 3.6$$

$$r = \frac{\omega}{\omega_n} \quad Equation\ 3.7$$

$$\omega_d = \omega_n \sqrt{1 - \varepsilon^2} \quad Equation\ 3.8$$

Table 8: Standard Values

k	6060.1 N/m
$\mathbf{F_o}$	120 N
$\boldsymbol{\omega}$	104.7 rad/s
$\boldsymbol{\omega_n}$	560.35 rad/s
$\boldsymbol{\omega_d}$	560.3 rad/s
$\boldsymbol{\delta}$	0.0198

Since the given system is under damped (Table 5) so the total response is given as:

$$x(t) = X_o e^{-\delta\omega_n t}\cos(\omega_d t - \varphi_o) + Xcos(\omega t - \varphi) \qquad Equation\ 3.9$$

Where

$$X = \frac{\delta}{\sqrt{(1-r^2)^2+(2\delta r)^2}} \qquad Equation\ 3.10$$

$$tan\varphi = \frac{2\delta r}{1-r^2}$$

Similarly

$$x_o = X_o\, cos\varphi_o + Xcos\varphi \qquad Equation\ 3.11$$

$$\dot{x}_0 = -\delta\omega_n X_o cos\varphi_o + \dot{\omega}_d X_o sin\varphi_o + \omega X sin\varphi \qquad Equation\ 3.12$$

$Equation\ 3.4$

Solving above two equation simultaneously and putting in Equation 3.9

$$\boldsymbol{x(t) = 0.00359e^{-1.12t}\cos(560.3t - 0.002136) + 0.00299\cos(104.7t - 0.00074)}$$

Pressure Calculations

Pressure that the syringe plunger puts on the binder is calculated using Hagen-Poiseuille Equation for a laminar flow in a constant area pipe. The syringe needle can be analyzed as a constant area pipe

$$Flow\ rate = AV = \frac{\pi r^4 (P - P_0)}{8\mu l} \qquad Equation\ 4.0$$

Table 9: Cylinder Injection Parameters

Parameter	Notation	Value
Length of needle	l	38 mm
Dynamic viscosity of binder	μ	4.62 cp
Inner radius of needle	R	0.255 mm
Atmospheric pressure	P_0	101325 pa

Plunger Pressure can then be calculated for required velocity at the output

$$P = \frac{V}{4.6298 \text{ x } 10^{-5}} + P_0 \qquad Equation\ 4.1$$

Reynolds number at the outlet is also calculated as:

$$R_e = \frac{\rho V d}{\mu} \qquad Equation\ 4.2$$

The velocity of the binder is calculated in the following way:

The area of binder jet which leaves the needle is

$$\text{Jet Area} = \pi * (radius\ of\ jet)^2 \qquad Equation\ 4.3$$

where the jet radius is equal to the inner radius of needle. So, we get a jet area of 0.204mm^2

The volume of binder required to be dispensed on the total surface of print bed is calculated as

Volume of binder= bed length * bed width * sand layer thickness

Volume= 126.45 mm^3

Where sand layer thickness is considered because of the assumption that binder reaches to the base of a sand layer which makes the thickness of binder layer equal to sand layer thickness. The time requirement for the binder to set is 1 min, which means that the volume flow rate must be

Volume flow rate to dispense binder on all the bed in 1 min= 2.1075 mm^3/s

Now this flow rate can be compared with the flow rate inside the needle by which we can find the velocity of binder at the exit to be

Binder velocity at the outlet= Volume flow rate/ inner area of needle

Binder velocity= 5.158 mm/s

Reynolds number for a velocity of 0.01 m/s corresponds to:

$$R_e = 1.247$$

Velocity and Pressure Contours

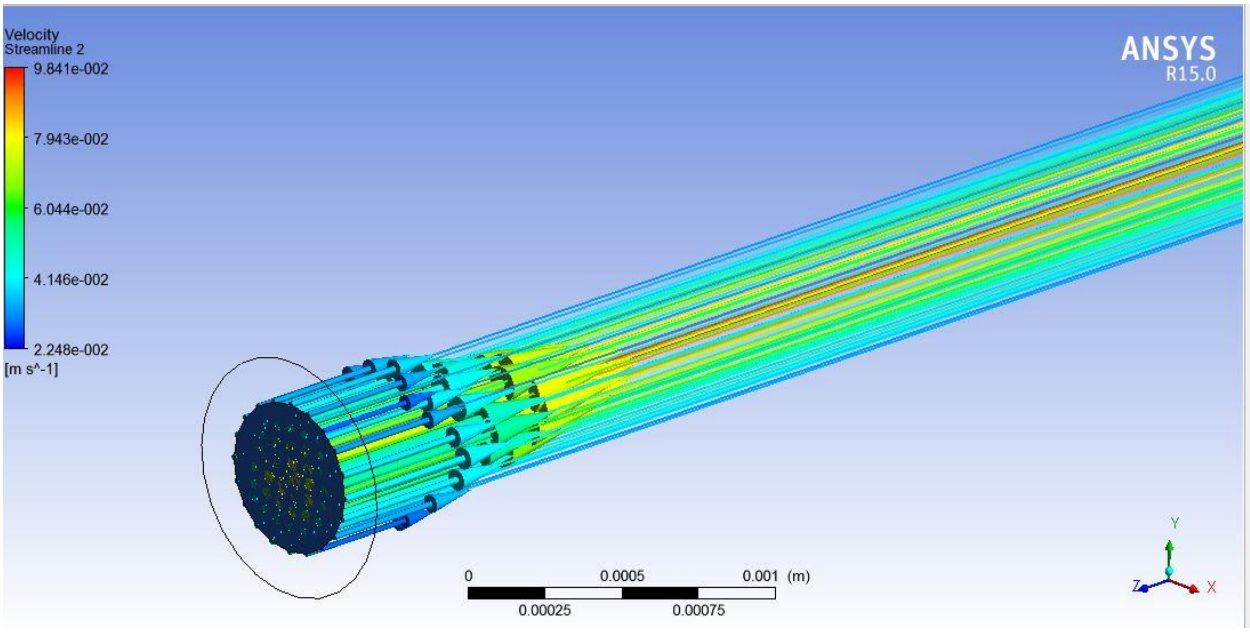

Figure 26: Outlet Velocity Contour

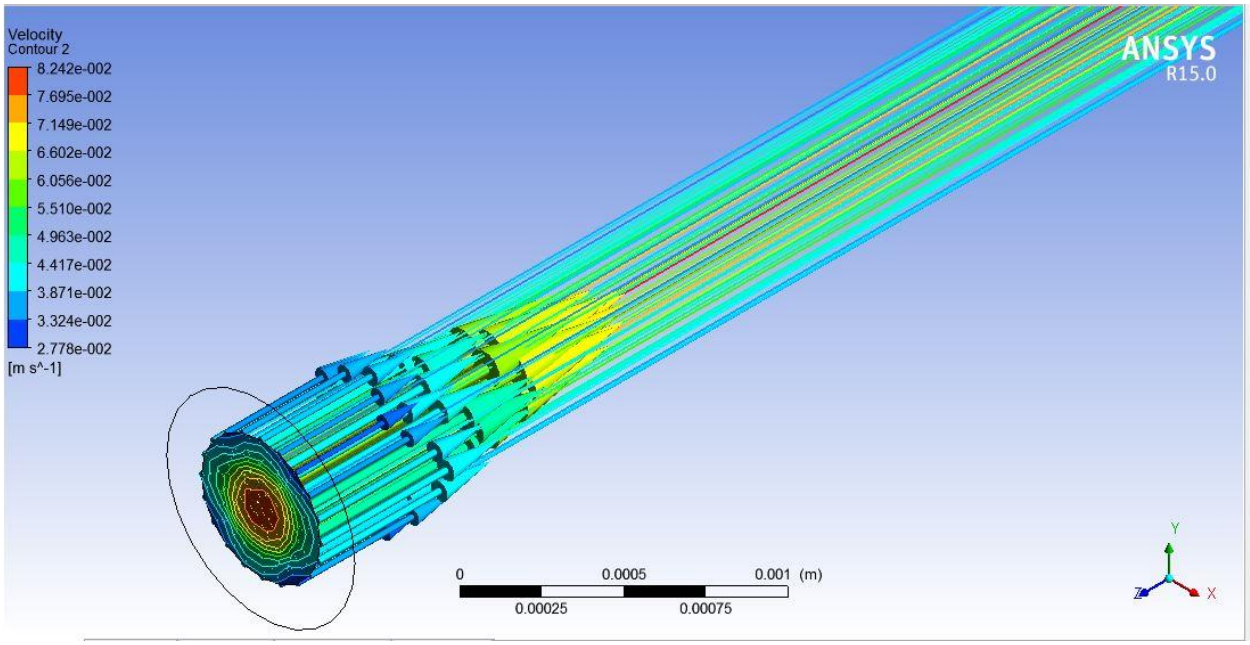

Figure 27: Inlet Velocity Contour

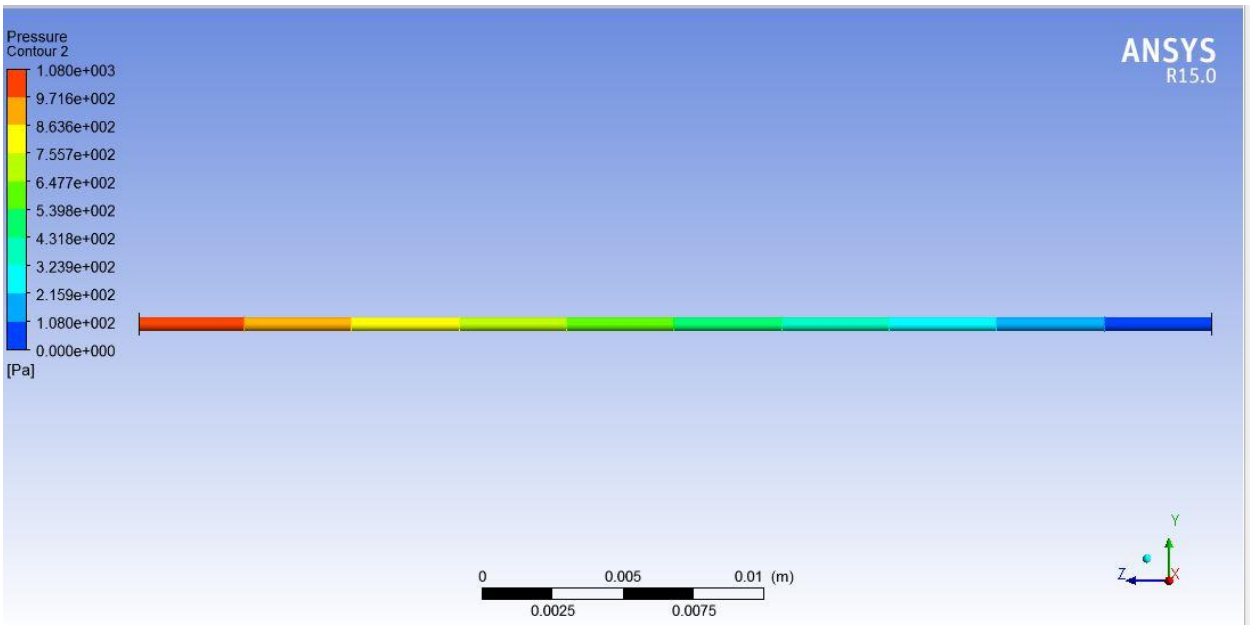

Figure 28: Pressure Contour

Transient Response of Bed

To check transient of the system during movement, ANSYS is used and initial parameters that needs to be defined:

- Pressure on the plate
- Velocity of the plate
- Lifting force

Since velocity is given by

$$V = \frac{s}{t} \qquad Equation\ 5.0$$

Where S is the distance covered in z-axis and is equal to thickness of sand layer which means;

S=0.4mm. This required height is achieved in10 steps; time for this required height is calculated from motor RPM

At 1000 RPM

1000 revolutions in 1 minute

Since motor covers one revolution in 200 steps

1000 x 200 step completed in 60 seconds

$$\text{10 steps completed in} = \frac{60}{1000 \text{ x } 200} \text{ x } 10 \qquad Equation\ 5.1$$

Time = 0.003 seconds

$$\text{Velocity} = \frac{0.4 \text{ x } 10^{-3}}{0.003} \qquad Equation\ 5.2$$

$$\mathbf{V = 0.1\ \frac{m}{s}}$$

$$\text{Pressure is calculated as : } P = \frac{70.53}{0.1778 \text{ x } 0.1778} \qquad Equation\ 5.3$$

P = 2231 Pa

Lifting force is calculated from motor Torque at 300 RPM

T= 0.2812 Nm at 300 rpm

$$F = \frac{0..2812}{0.004}$$ **F=70.53 N** on single screw

Lifting force = **70.53N.** With the definition of system parameters ANSYS transient response was calculated and results are as follows:

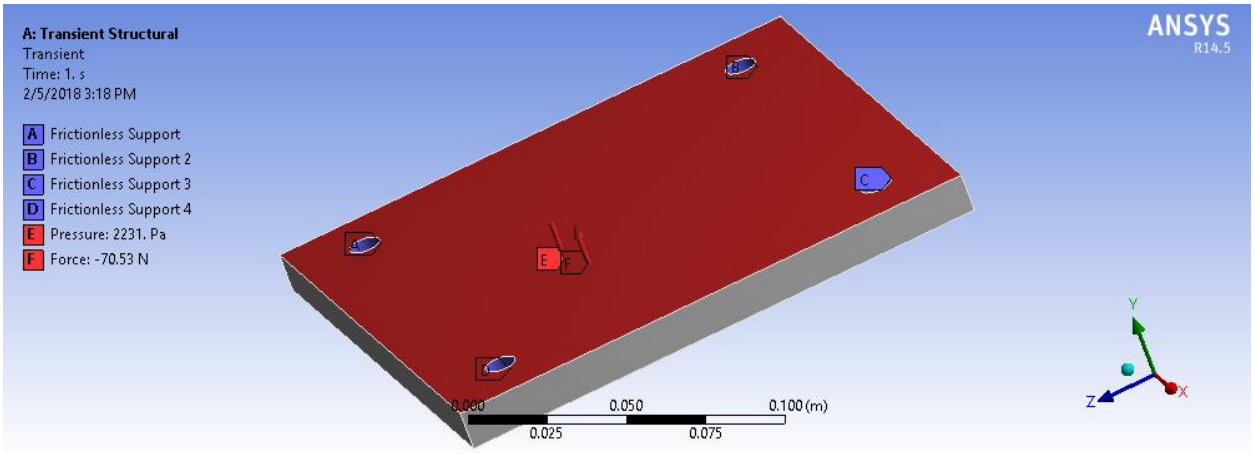

Figure 29: Boundary Conditions transient response

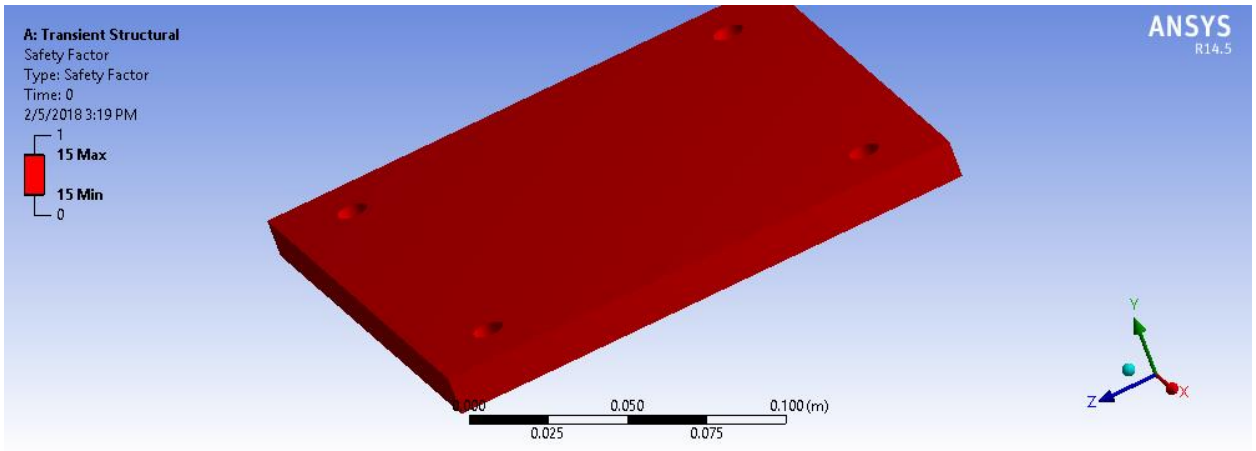

Figure 30: Safety factor

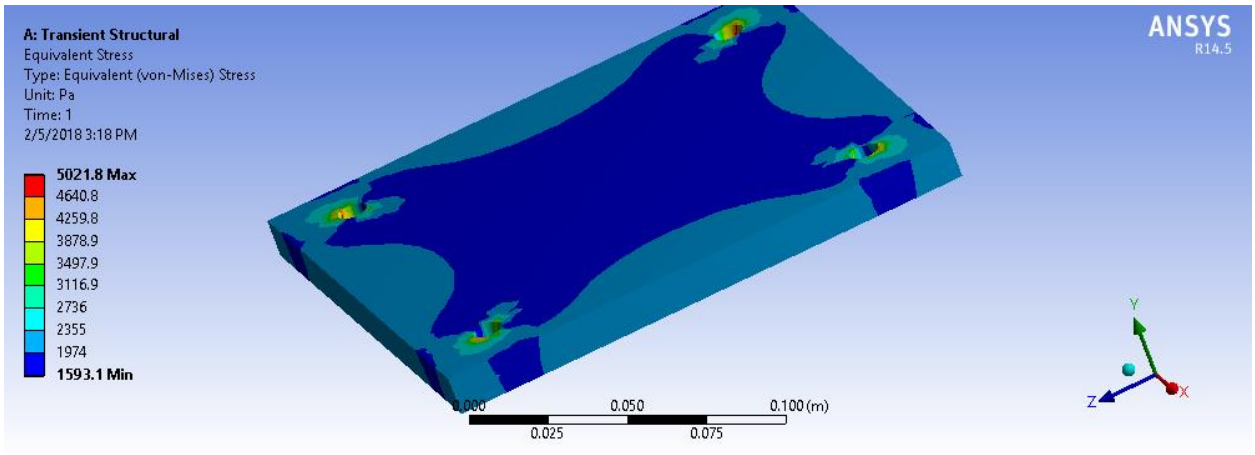

Figure 31: Von mises Stress

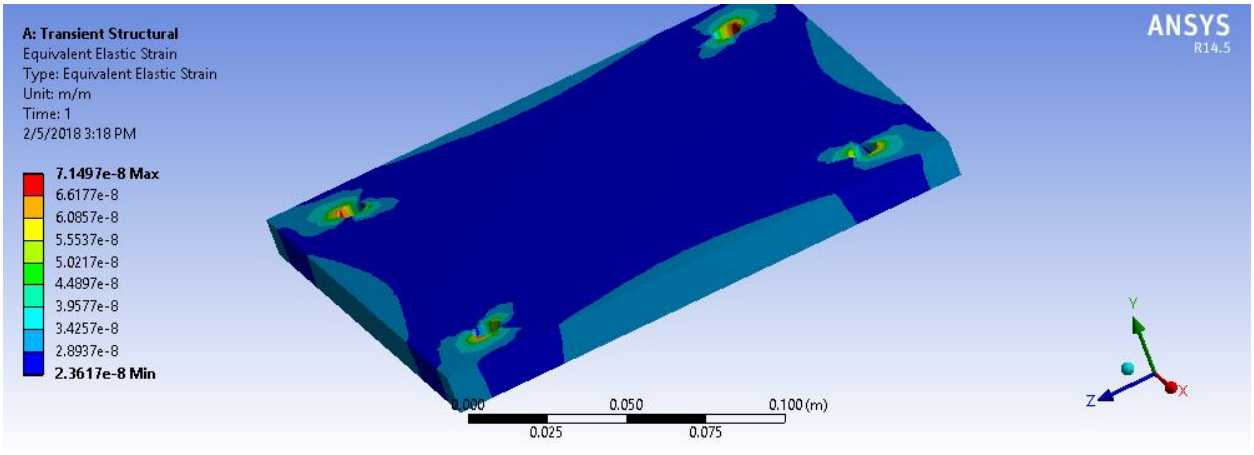

Figure 32: Von Mises Strain

Arduino Code

The arduino code developed for the running of the prototype is as follows:

```
#define X_STEP_PIN 54
#define X_DIR_PIN 55
#define X_ENABLE_PIN 38
#define X_MIN_PIN 3
#define X_MAX_PIN 2

#define Y_STEP_PIN 60
#define Y_DIR_PIN 61
#define Y_ENABLE_PIN 56
#define Y_MIN_PIN 14
#define Y_MAX_PIN 15

#define Z_STEP_PIN 46
#define Z_DIR_PIN 48
#define Z_ENABLE_PIN 62
#define Z_MIN_PIN 18
#define Z_MAX_PIN 19

#define E_STEP_PIN 26
#define E_DIR_PIN 28
#define E_ENABLE_PIN 24

#define Q_STEP_PIN 36
#define Q_DIR_PIN 34
#define Q_ENABLE_PIN 30
```

```
#define SDPOWER -1
#define SDSS 53
#define LED_PIN 13
#define FAN_PIN 9
#define PS_ON_PIN 12
#define KILL_PIN -1
#define HEATER_0_PIN 10
#define HEATER_1_PIN 8
#define TEMP_0_PIN 13


int xcounter = 1, ycounter = 1, counter = 0;
boolean s1 = HIGH, s2 = HIGH, s3 = HIGH, s4 = HIGH;

void setup() {
  Serial.begin(115200);
  pinMode(FAN_PIN , OUTPUT);
  pinMode(HEATER_0_PIN , OUTPUT);
  pinMode(HEATER_1_PIN , OUTPUT);
  pinMode(LED_PIN , OUTPUT);
  pinMode(X_STEP_PIN , OUTPUT);
  pinMode(X_DIR_PIN , OUTPUT);
  pinMode(X_ENABLE_PIN , OUTPUT);
  pinMode(Y_STEP_PIN , OUTPUT);
  pinMode(Y_DIR_PIN , OUTPUT);
  pinMode(Y_ENABLE_PIN , OUTPUT);
  pinMode(Z_STEP_PIN , OUTPUT);
```

```
pinMode(Z_DIR_PIN , OUTPUT);
pinMode(Z_ENABLE_PIN , OUTPUT);
pinMode(E_STEP_PIN , OUTPUT);
pinMode(E_DIR_PIN , OUTPUT);
pinMode(E_ENABLE_PIN , OUTPUT);
pinMode(Q_STEP_PIN , OUTPUT);
pinMode(Q_DIR_PIN , OUTPUT);
pinMode(Q_ENABLE_PIN , OUTPUT);
digitalWrite(X_ENABLE_PIN , LOW);
digitalWrite(Y_ENABLE_PIN , LOW);
digitalWrite(Z_ENABLE_PIN , LOW);
digitalWrite(E_ENABLE_PIN , LOW);
digitalWrite(Q_ENABLE_PIN , LOW);

pinMode(16 , OUTPUT);
pinMode(17 , OUTPUT);
pinMode(25 , OUTPUT);
pinMode(27 , OUTPUT);


pinMode(23 , INPUT);
pinMode(29 , INPUT);

digitalWrite(16 , HIGH);
digitalWrite(17 , LOW);
digitalWrite(25 , HIGH);
digitalWrite(27 , LOW);
```

```
for (int i = 0; i < 3500; i++)
{
  digitalWrite(Y_DIR_PIN, HIGH);
  digitalWrite(Y_STEP_PIN, s1);
  s1 = !s1;
  delay(2);
}
delay(1000);
for (int i = 0; i < 300; i++)
{
  digitalWrite(E_DIR_PIN, LOW);
  digitalWrite(E_STEP_PIN, s1);
  s1 = !s1;
  delay(2);
}
delay(1000);
while (digitalRead(23) == HIGH)
{
  digitalWrite(X_DIR_PIN, HIGH);
  digitalWrite(X_STEP_PIN, s1);
  s1 = !s1;
  delayMicroseconds(1000);
}

//    for (int i = 0; i < 2000; i++)
//    {
//      digitalWrite(E_DIR_PIN, HIGH);
//      digitalWrite(E_STEP_PIN, s1);
```

```
  //      s1 = !s1;
  //      delayMicroseconds(2000);
  //    }
  for (int i = 0; i < 200; i++)
  {
    digitalWrite(X_DIR_PIN, LOW);
    digitalWrite(X_STEP_PIN, s1);
    s1 = !s1;
    delayMicroseconds(1000);
  }
  for (int i = 0; i < 1200; i++)
  {
    digitalWrite(Y_DIR_PIN, LOW);
    digitalWrite(Y_STEP_PIN, s2);
    s2 = !s2;
    delay(1);
  }
  delay(1000);

}
int temp = 1;
void loop() {
  int steps;
  while (xcounter < 500)
  {
    if (temp == 1)
    {
      steps = 700;
```

```
  }
  else
  {
    steps = 100;
  }
  for (int i = 0; i < steps; i++)
  {
    temp++;
    digitalWrite(Q_DIR_PIN, HIGH);
    digitalWrite(Q_STEP_PIN, s1);
    s1 = !s1;
    delayMicroseconds(12000);
  }
  delay(2000);
  for (int i = 0; i < 25; i++)
  {
    digitalWrite(X_DIR_PIN, LOW);
    digitalWrite(X_STEP_PIN, s1);
    s1 = !s1;
    delayMicroseconds(1000);
    xcounter++;
  }
  delay(1000);
}
xcounter = 1;

for (int i = 0; i < 50; i++)
{
```

```
  digitalWrite(Y_DIR_PIN, LOW);
  digitalWrite(Y_STEP_PIN, s2);
  s2 = !s2;
  ycounter++;
  delay(2);
}

for (int i = 0; i < 500; i++)
{
  digitalWrite(X_DIR_PIN, HIGH);
  digitalWrite(X_STEP_PIN, s1);
  s1 = !s1;
  delayMicroseconds(2000);
}

if (ycounter >= 500)
{
  for (int i = 0; i < 100; i++)
  {
    digitalWrite(X_DIR_PIN, HIGH);
    digitalWrite(X_STEP_PIN, s1);
    s1 = !s1;
    delayMicroseconds(1000);
  }
  delay(1000);
  for (int i = 0; i < 1750; i++)
  {
    digitalWrite(Y_DIR_PIN, LOW);
```

```
  digitalWrite(Y_STEP_PIN, s2);
  s2 = !s2;
  ycounter++;
  delay(1);
}
delay(6000);

for (int i = 0; i < 3500; i++)
{
  digitalWrite(Y_DIR_PIN, HIGH);
  digitalWrite(Y_STEP_PIN, s1);
  s1 = !s1;
  delay(2);
}
delay(1000);
for (int i = 0; i < 300; i++)
{
  digitalWrite(E_DIR_PIN, LOW);
  digitalWrite(E_STEP_PIN, s1);
  s1 = !s1;
  delay(2);
}
delay(1000);
while (digitalRead(23) == HIGH)
{
  digitalWrite(X_DIR_PIN, HIGH);
  digitalWrite(X_STEP_PIN, s1);
  s1 = !s1;
```

```
    delayMicroseconds(1000);
   }
   for (int i = 0; i < 200; i++)
   {
    digitalWrite(X_DIR_PIN, LOW);
    digitalWrite(X_STEP_PIN, s1);
    s1 = !s1;
    delayMicroseconds(1000);
   }
   for (int i = 0; i < 1200; i++)
   {
    digitalWrite(Y_DIR_PIN, LOW);
    digitalWrite(Y_STEP_PIN, s2);
    s2 = !s2;
    delay(1);
   }
   delay(1000);
   ycounter = 1;
  }
}
```

CHAPTER 4: RESULTS AND DISCUSSION

The elevation in sand beds is very small nearly equal to 0.4 mm. such precise elevation can only be achieved through stepper motors that operates in steps and covers a very small distance in each step. For selection of particular stepper motor fit for our model, torque required in lifting and lowering the Feed and print beds are calculated respectively.

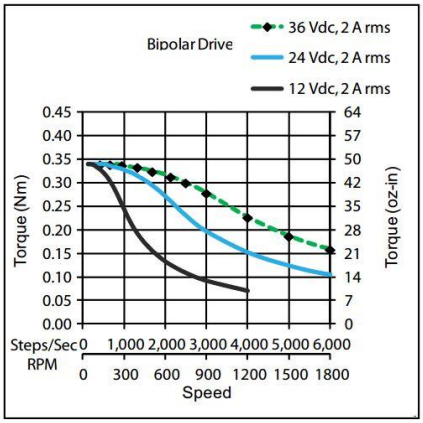

Figure 33: Torque vs. RPM

Both value of torques lie in the range of common NEMA 17 stepper motor. The torque of these motors is function of motor's speed. Motor can be driven at different speed generally ranging from 0 to 1800 rpm.

Required torque is achieved by driving motor from 300 to 600 rpm which corresponds to.

Torque acts in the direction of lead screw's lead and force due to motor's rotor acting on the screw is calculated to be used in vibrational analysis.

Typical steps in one revolution are 200 but further micro stepping can be made using programmable arduino and trigorilla control board.

In our case no further micro stepping is required as the required elevation is easily achieved in 10 steps of motor.

All motors are controlled using arduino control board which is programmed though PC.

Due to applied load on the screw our lead screw may fail due to the compressive stress and may even buckle under the load. For safe operation the screw should not buckle or fail due to stresses

Next step was the calculation compressive stress and buckling of the screw under the load to be lifted.

The stress on the screw is within the safe limit of yield strength of steel which is 250 MPa and stress on our screw is just 1.76 MPa, which proves that the screw is completely safe from failure due to stress.

Force applied on the screw is also within the safe limit for buckling. Our screw will buckle at approx 337 N whereas the force applied is just 50 N so the screw is in safe limit and will not buckle.

Stress and deflection analysis of stress and strain developed in sand beds as a result of sand weight acting on them. For safe operation of the printer the beds should be able to withstand any particular stresses applied on them. A very simple and systematic approach was to consider the plate of bed and calculation of stresses was carried out using both simple derived equations for stress and deflection and ANSYS.

Different materials were tested mainly the most common manufacturing ones that include Aluminum, Stainless steel and cast iron. Stress and deflection analysis shows very little deflection in each material. ANSYS analysis of stress revealed that each material is perfectly safe to operate.

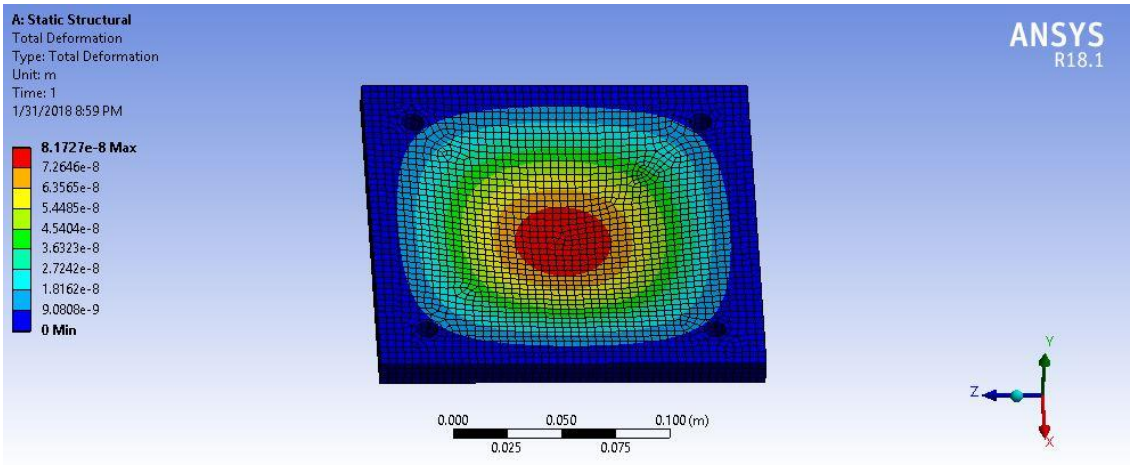

Figure 34: Aluminum deflection

Displacement analysis of bed with supporting plate shows a very little deformation which is easily negligible.

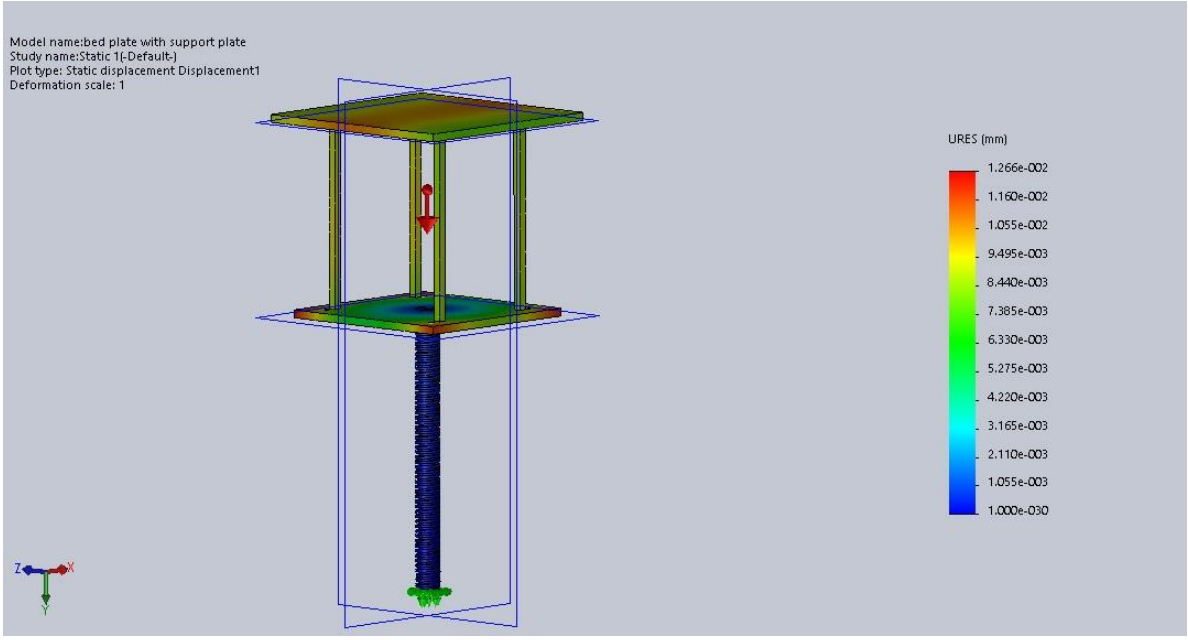

Figure 35: Bed Deformation

Final selection of Aluminum is based on its:

- Better thermal conductivity
- Cost effectiveness
- Lighter material.

Aluminum is lighter than the other two competitors, which reduces overall weight on the lead screws and has greater thermal conductivity that is in favor of print bed heater, more over aluminum is cheapest among all and hence Aluminum is selected for manufacturing.

Vibrational analysis of the bed is done to see the response of the system under natural oscillations as well as under the influence of harmonic force

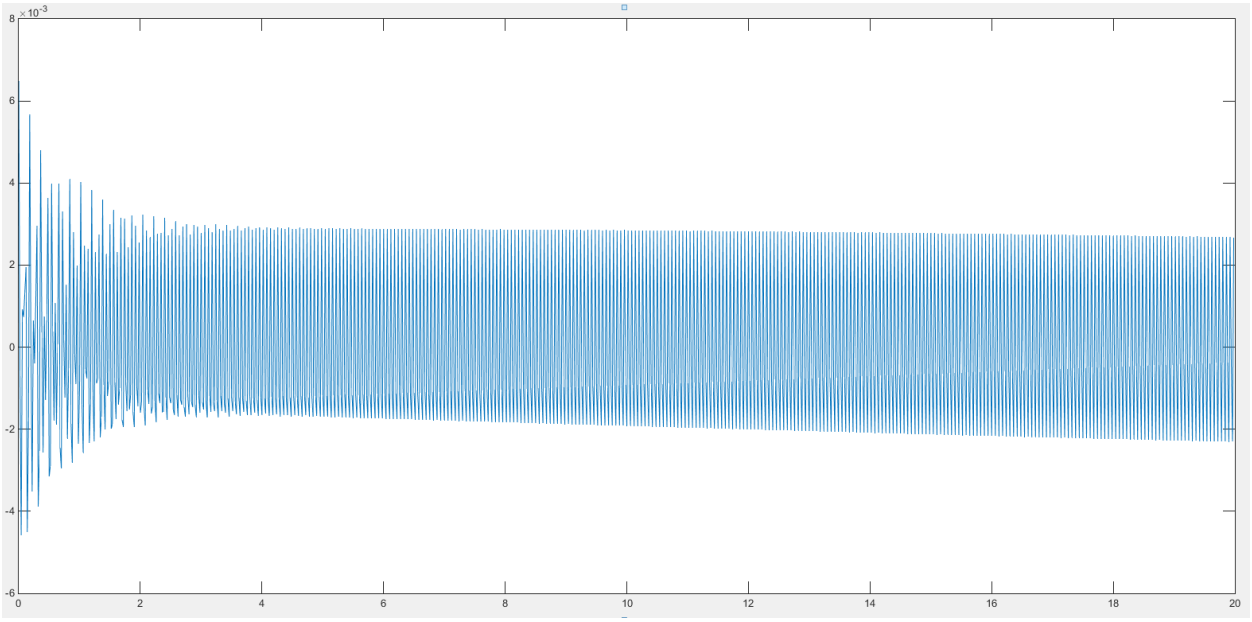

Figure 36: System vibration response

System response shows that in start bed oscillates with natural frequency response and forced harmonic response but with passage of time natural response decays due to material damping while oscillations remain only due to harmonic force which is very minute nearly equal to 2×10^{-3} mm which can be safely neglected.

Overall response shows very little vibrations in the system which will not affect the functioning of the printer, as the bed is brought to complete stop when binder is displaced.

Neglecting any pressure drop in the syringe the pressure at the outlet is nearly equal to pressure at the inlet which is provided to the syringe by the plunger system. To calculate that pressure required, pressure at the outlet was calculated using most suitable velocity. Velocity range from 0.01 m/s to 0.03 m/s to avoid choking and achieve required accuracy keeping in mind the setting time of the binder. The velocity found from the calculations i.e.: .01m/s is for the binder to dispense on all the surface area on the print bead in 1 min. If the setting time of binder varies, the velocity will be changed in order to have a good mold strength.

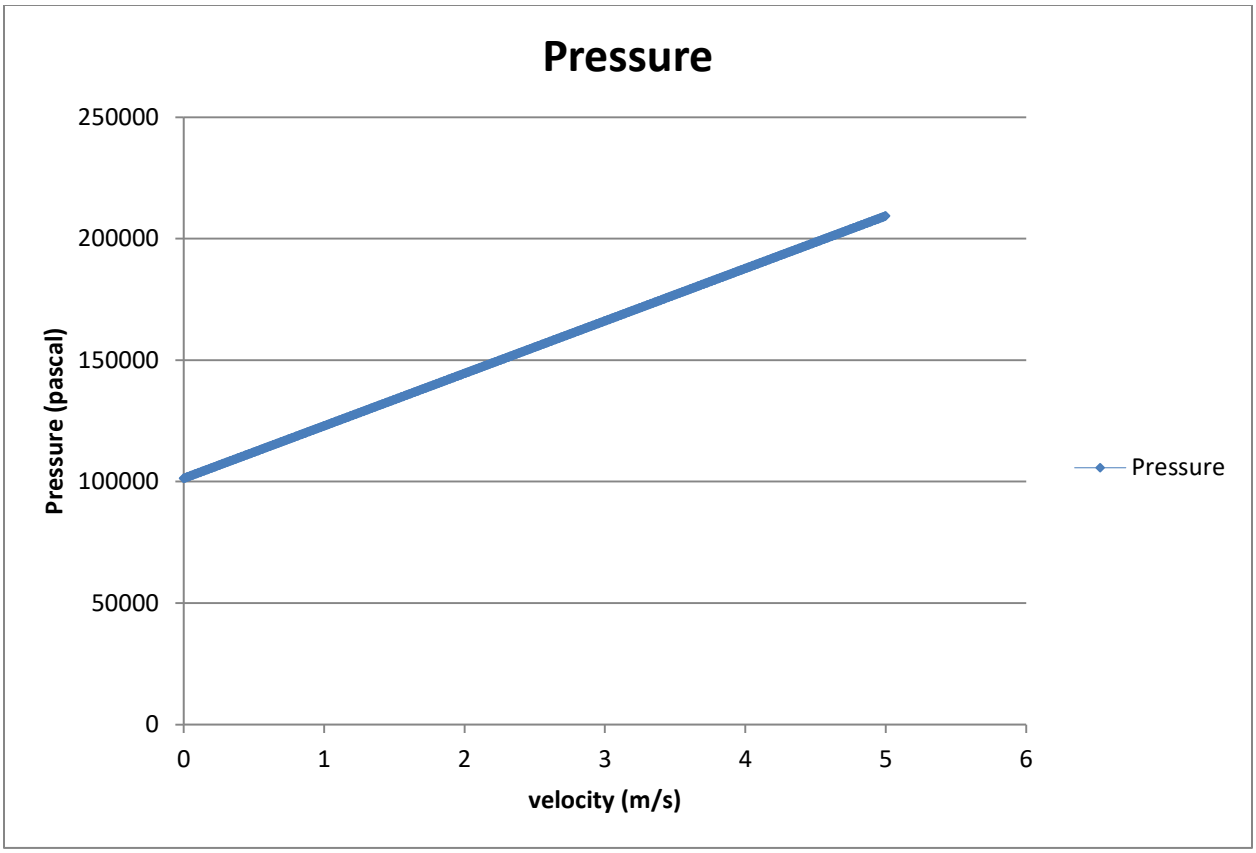

Figure 37: Pressure velocity graph

Pressure corresponding to this velocity range lies between **101540.992 Pa** to **101972.9762 Pa.**

The velocity of fluid inside the pipe varies in two manners, one in the radial direction and the other in the axial direction. The flow of furfural alcohol in the needle was approximated as the fluid flow in a circular pipe with constant diameter

The Pressure and velocity contours for maximum ranges of fluid velocity are shown. Fluid velocity in the radial direction changes from an upper limit of approximately 0.084 m/s to a lower velocity of approximately 0.022 m/s. As it is quite evident that the velocity around the centerline of a constant area pipe will be larger than the fluid velocity near the pipe walls from velocity contours. The change in fluid velocity is due to the wall shear force which is different for different flow regimes but for a laminar flow the velocity has a linear profile. Due to the

velocity profile the fluid velocity changes radially. The arrow heads along with the stream lines, both in different color ranges show that fluid particles at the center will move faster as compared to the particles moving near the wall.

The difference in the upper and lower velocity ranges in outer velocity contour and inner velocity contour show that the fluid velocity increases in the flow direction. The increase in velocity is due to reduction in pressure in the axial direction. Velocity increases both near the wall and the centerline. The upper range of velocity in the outer contour is almost 0.0987 m/s while the lower velocity is 0.0224 m/s. The change in velocity in the radial direction is neglected because of a smaller size of needle. Due to the smaller size, the difference in velocity can be approximated as an average velocity which will be taken as a constant value along the radius of needle. The average value at the outlet is near to 0.055 m/s (maximum allowable velocity) which is relatively bigger than our required value of 0.01-0.03 m/s to dispense binder on the sand in a uniform manner. The Pressure at the inlet required for an outlet velocity of 0.05 m/s is 1079 Pa (Gauge Pressure) from the Hagen-Poiseuille Equation and that found from the pressure contours is 1080 Pa. This value of pressure justifies the use of Hagen-Poiseuille Equation for a laminar flow in a circular pipe. The little difference in two values is due to the fact that above mentioned equation does not include the effect of the wall shear and the simulations done in ANSYS incorporates the wall shear and velocity profile. As the difference in the two values is not very large, the values found from Hagen-Poiseuille Equation can be used for further calculations.

From the pressure contour it is apparent that the gauge pressure decreases in the flow direction from the pressure at the inlet to the atmospheric pressure at the exit. The pressure changes linearly and causes the fluid velocity to increase in the same direction.

The Reynolds number for 0.01 m/s is 1.247 which proves that the flow in the needle is indeed laminar and the assumptions made about the fluid are justified which included the use of the Hagen-Poiseuille Equation for laminar flow of a viscous fluid and the approximation of needle as a constant area pipe.

Further movement of bed with constant velocity against under load of sand requires verification of transient response of the system to be in safe limit,

To prove that, transient response of the bed is carried out on ANSYS for vertical movement with pressure on the surface resulting from the weight load and for the given velocity and lifting force, it was quite evident that lifting force is enough to provide the necessary elevation with the given velocity.

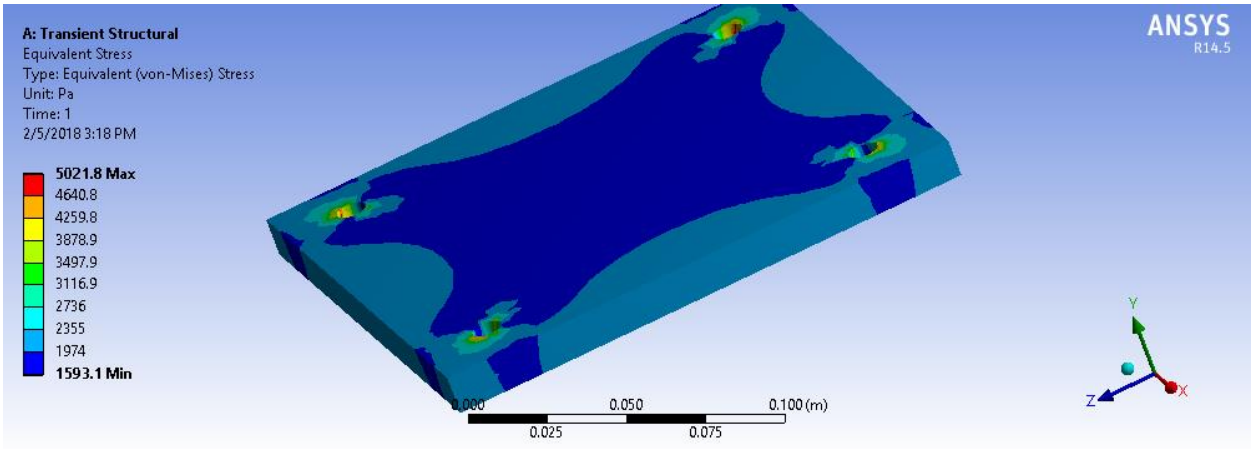

Figure 38: Von mises Stress

Similarly von mises Stress analysis reveals that during whole operation bed moves with constant velocity and with the above given stress distribution it is clearly evident that bed does not face deflection in the shape and is immune to failure.

The speed of curing reaction be brought up to 3 minutes with appropriate mixing of phenolic binder with high acidity and speed hardener to reach appropriate curing as compared to the other ones in figure and . The phenolic binder was chosen to its added advantages along with cost and availability. Figure 39 shows that at room temperatures, the binders curing can be reached up to 2 mins. The binder and hardener grades are used in advised proportions. Figure 40 and 41 depict the stripping time for lesser grade hardners.The maintained temperature is high and the rate is slower. Hence we'll initially go forward employing phenolic binder initially.

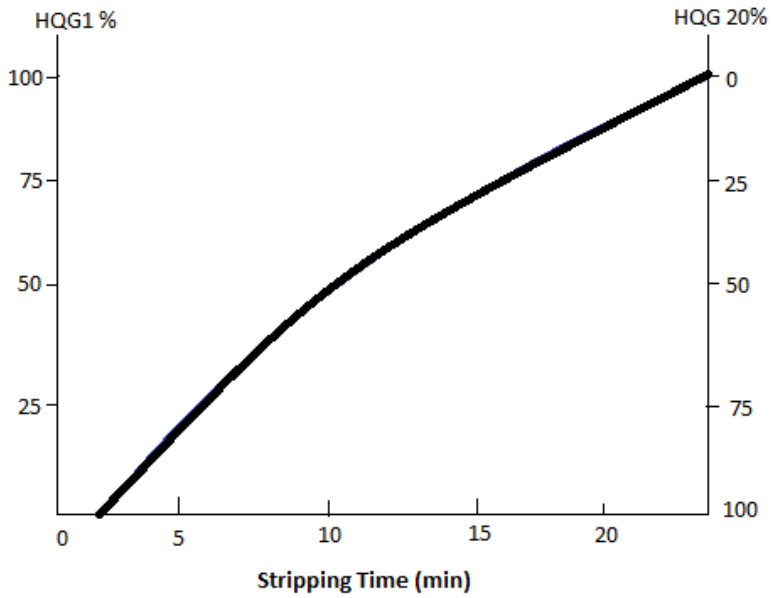

Figure 39 : Stripping time reduction (1)

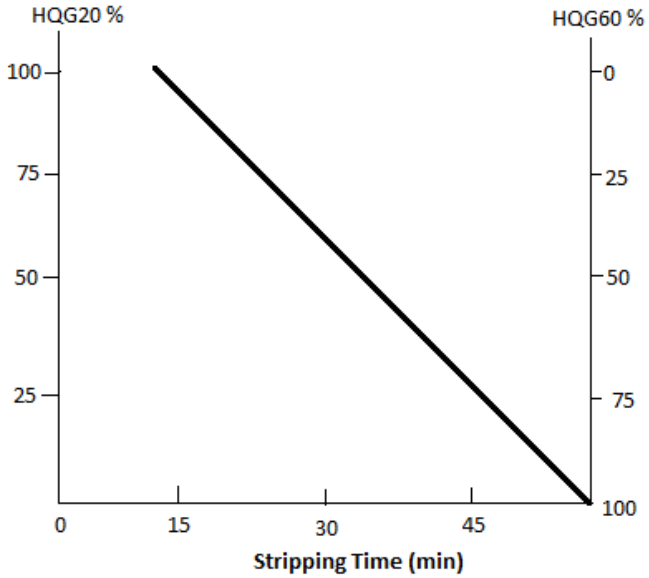

Figure 40: Stripping Time (2)

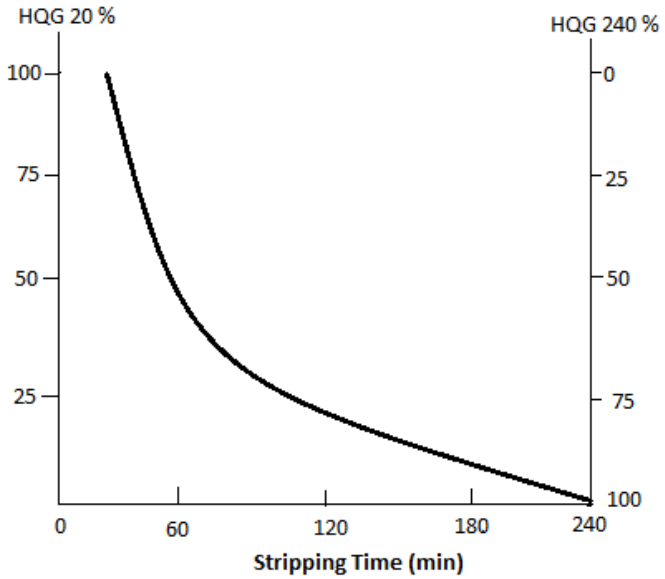

Figure 41: Stripping Time (3)

CHAPTER 5: CONCLUSIONS AND RECCOMENDATIONS

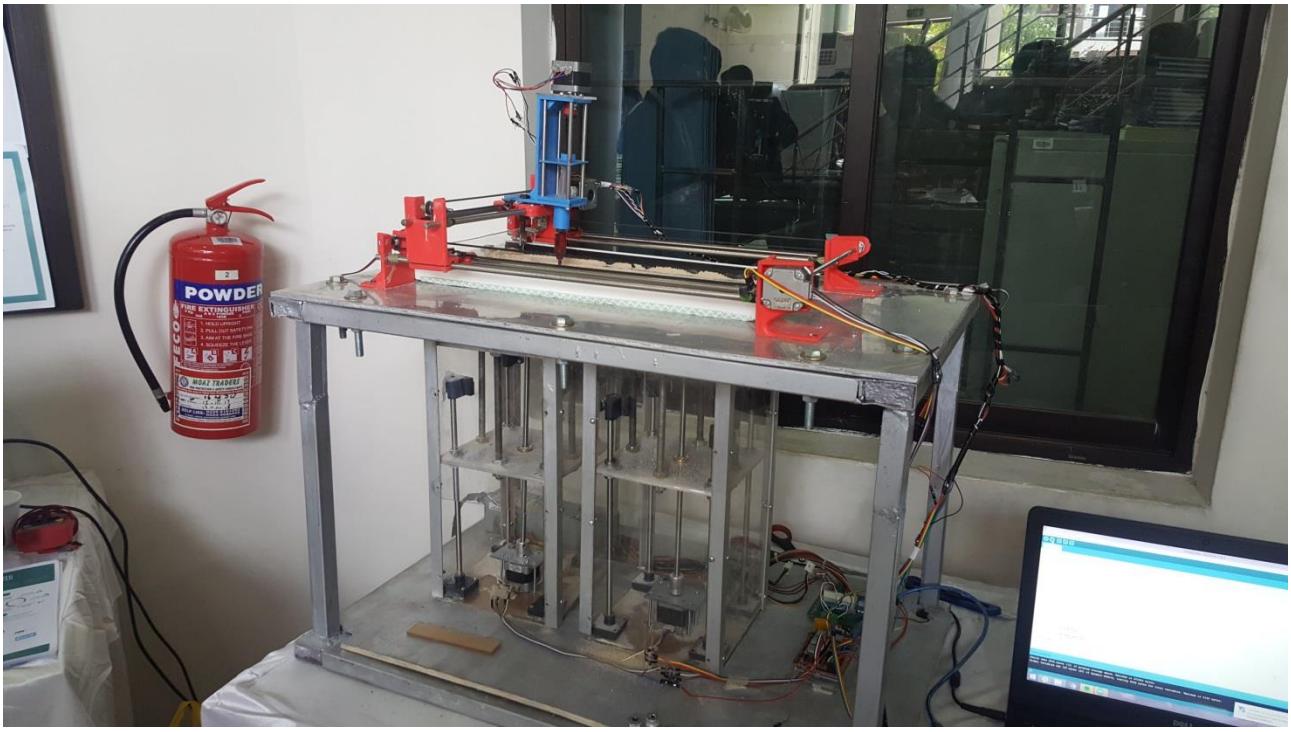

Figure 42: 3D Sand Mold Printer Prototype

The first mold that was constructed by the prototype was a 4x 4x 2.5-inch cubic mold and the second attempt (in figure 43) was 1.5 x 1.5 x 1 inch cube. The time it for the mold to set and harden was 40 minutes. The mold was contracted from layer by layer deposition of sand, this was achieved by lifting the print bed to achieve 6mm layer thickness. The binder was dispensed using a syringe nozzle with a syringe pump assembly carefully attached. The amount of binder used in the syringe is 5ml. The amount of sand in the feed bed was 3 kg and the amount of sand in the print bed was 2 kg. The mold layer settled in 2 minutes time and the dispensing of each layer took 1 minute. The strength of the mold was assessed using the wet sand mold hardness tester.

Figure 43: Mold Example Printed with Prototype

Its calibrated value came around to be 87 whereas 60-70 is the industrial standard value.
The prototype in its present state is inhibited by the dimensional inaccuracy due to the usage of syringe pump. The surface tension of the binder droplets between themselves also deter the accuracy with which the drops are dispensed. The drops are attracted towards the already spread-out binder drop on the sand due to surface tension which prevents the drop from being dispensed at the precise location.
We also used an aluminum plate on the prototype's frame, which added excessively to the weight of the prototype as a whole. The refilling of the syringe was also an issue, as its head had to be removed manually and then fill the syringe accordingly.
We didn't incorporate greater geometrical complexity due to the usage of syringe nozzle

Future Recommendations:

After carefully concluding the results and discussion about the 3D sand printer, we can suggest the following future recommendations

1- The syringe that is being used for dispensing the binder can be replaced with a piezoelectric printhead thus increasing the resolution of printing and it will also make the printing of complex geometries easier.

2- The size and capacity of both the beds can be increased to make bigger molds.

3- The printer can be used for printing of artworks as well by replacing the sand and phenolic binder with ceramic powder and relative binder respectively.

4- The scraper for scraping of the sand from feed bed to print bed can be replaced with a roller to introduce compaction which will increase the mold strength.

5- The mold strength can also be increased by heating the sand by installing heaters in the beds.

References

[1] Sachs, Emanuel, et al. "Three dimensional printing: rapid tooling and prototypes directly from a CAD model." Journal of Engineering for Industry 114.4 (1992): 481-488..

[2] ISO, ASTM. "Standard Terminology for Additive Manufacturing–General Principles–Terminology." (2015).

[3] Upadhyay, Meet, Tharmalingam Sivarupan, and Mohamed El Mansori. "3D printing for rapid sand casting—A review." Journal of Manufacturing Processes 29 (2017): 211-220.

[4] Wong KV, Hernandez A. A review of additive manufacturing. ISRN Mech Eng2012;2012:1–10, http://dx.doi.org/10.5402/2012/208760

[5] Bak, David. "Rapid prototyping or rapid production? 3D printing processes move industry towards the latter." Assembly Automation 23.4 (2003): 340-345.

[6] Dimitrov, Dimitar, Kristiaan Schreve, and Neal de Beer. "Advances in three dimensional printing–state of the art and future perspectives." Rapid Prototyping Journal 12.3 (2006): 136-147.

[7] Meteyer, Simon, et al. "Energy and material flow analysis of binder-jetting additive manufacturing processes." Procedia CIRP 15 (2014): 19-25.

[8] Gill, Simranpreet Singh, and Munish Kaplas. "Comparative study of 3D printing technologies for rapid casting of aluminium alloy." Materials and Manufacturing Processes 24.12 (2009): 1405-1411.

[9] Kruth, Jean-Pierre, et al. "Binding mechanisms in selective laser sintering and selective laser melting." Rapid prototyping journal 11.1 (2005): 26-36.

[10] Vaezi, Mohammad, and Chee Kai Chua. "Effects of layer thickness and binder saturation level parameters on 3D printing process." The International Journal of Advanced Manufacturing Technology 53.1-4 (2011): 275-284.

[11] McKenna, Nicholas, et al. "Direct Metal casting through 3D printing: A critical analysis of the mould characteristics." Global Congress on Manufacturing and Management (GCMM) Board, 2008.

[12] Snelling, Dean, Christopher Williams, and Alan Druschitz. "A comparison of binder burnout and mechanical characteristics of printed and chemically bonded sand molds." SFF Symposium, Austin, TX. 2014.

[13] Tóth, Judit, et al. "Heat absorption capacity and binder degradation characteristics of 3D printed cores investigated by inverse fourier thermal analysis." International Journal of Metalcasting 10.3 (2016): 306-314.

[14] Chhabra, M., and R. Singh. "Mathematical modeling of surface roughness of castings produced using ZCast direct metal casting." Journal of The Institution of Engineers (India): Series C 96.2 (2015): 145-155.

[15] Snelling, Dean, et al. "The effects of 3D printed molds on metal castings." International solid freeform fabrication symposium. 2013.

[16] Almaghariz, Eyad S., et al. "Quantifying the role of part design complexity in using 3D sand printing for molds and cores." International Journal of Metalcasting 10.3 (2016): 240-252.

[17] Ramakrishnan, Robert & Himmel, Benjamin & Volk, Wolfram & Günther, Daniel & Günther, Johannes. (2014). 3D Printing of Inorganic Sand Moulds for Casting Applications. Advanced Materials Research.

[18] Bobrowski, Artur, and Beata Grabowska. "The impact of temperature on furan resin and binders structure." Metallurgy and Foundry Engineering 38 (2012): 73-80.

[19] Abdul Rahid , Rastagar Engineering "Pakistan Metal Casting and Manufacturing Scene"

[20] Pham, Duc Truong, and Rosemary S. Gault. "A comparison of rapid prototyping technologies." International Journal of machine tools and manufacture 38.10-11 (1998): 1257-1287.

[21] ExOne. ExOne offers a variety of manufacturing quality materials that stand up to industrial use and easy integration into existing processes;http://www.exone.com/Resources/Materials

[22] Voxeljet Sand casting molds - Rapid and economical n.d. http://www.voxeljet.de/en/materials/sand/ (February 2, 2017).

[23] Mancusa Chemicals- Furan Process http://www.mancusochemicals.com/wp-content/uploads/2013/05/Furan.pdf

[24] Meteyer, Simon, et al. "Energy and material flow analysis of binder-jetting additive manufacturing processes." Procedia CIRP 15 (2014): 19-25.

[25] Throssell, Raymond W. "Stepper motor drive." U.S. Patent No. 4,283,672. 11 Aug. 1981.

[26] Yamano, Kenji, and Tetsuo Tamamura. "Fail-safe motor-driven cylinder for lifting apparatus." U.S. Patent No. 4,635,491. 13 Jan. 1987.

[27] Rao, Singiresu S. *Vibration of continuous systems*. John Wiley & Sons, 2007.

[28] Gooch, Jan W. "Hagen-Poiseuille equation." *Encyclopedic Dictionary of Polymers*. Springer New York, 2011. 355-355

[29] Loudon, Catherine, and Katherine McCulloh. "Application of the Hagen—Poiseuille Equation to Fluid Feeding through Short Tubes." Annals of the Entomological Society of America 92.1 (1999): 153-158.

[30] Kolmogorov, Andrey Nikolaevich. "The local structure of turbulence in incompressible viscous fluid for very large Reynolds numbers." Dokl. Akad. Nauk SSSR. Vol. 30. No. 4. 1941.

[31] Huang, R., Zhang, B. & Tang, Y. China Foundry (2016) 13: 231. https://doi.org/10.1007/s41230-016-6022-x

[32] Mancusa Chemicals – Phenolic Urethane Binder (2009)

[33] Sachs E, Cima M, Three-Dimensional Printing: Rapid Tooling Cornie J. Proto-types directly from a CAD model. CIRP Ann Manuf Technol 1990;39:201–4.

APPENDIX I : Modulus of Elasticity

Modulus of Elasticity Values for Metals		
Aluminum Alloys		
Metal	Modulus of Elasticity	
	GPa	10^6 psi
Aluminum Alloy 1100	69	10
Aluminum Alloy 2024	72.4	10.5
Aluminum Alloy 6061	69	10
Aluminum Alloy 7075	71	10.3
Aluminum Alloy 356.0	72.4	10.5

Cast Iron		
Metal	Modulus of Elasticity	
	GPa	10^6 psi
Gray Irons		
Grade G1800	66 - 97 *	9.6 - 14 *
Grade G3000	90 - 113 *	13.0 - 16.4 *
Grade G4000	110 - 138 *	16 - 20 *
Ductile Irons		
Grade 60-40-18	169	24.5
Grade 80-55-06	168	24.4
Grade 120-90-02	164	23.8

Steel Alloys		
Metal	Modulus of Elasticity	
	GPa	10^6 psi
Plain Carbon and Low Alloy Steels		
Steel Alloy A36	207	30
Steel Alloy 1020	207	30
Steel Alloy 1040	207	30
Steel Alloy 4140	207	30
Steel Alloy 4340	207	30
Stainless Steels		
Stainless Alloy 304	193	28
Stainless Alloy 316	193	28
Stainless Alloy 405	200	29
Stainless Alloy 440A	200	29
Stainless Alloy 17-7PH	204	29.5

APPENDIX II: LEAD SCREW SPECIFICATIONS

Lead Screw Product Availability

Metric

Dia. (mm) \ Lead (mm)	2	3	4	5	6	8	10	12	15	16	20	25	35	45
10	●	●		●	●		●				●		●	
12		●	●	●	●		●		●			●		●
16			●	●		●				●		●	●	
20			●			●		●		●	●			●
24				●										

● = stocked size

APPENDIX III: PROPERTIES OF FURAN

PHYSICAL PROPERTIES OF FURFURYL ALCOHOL

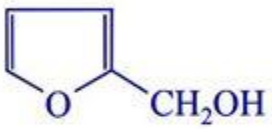

1.2 THERMODYNAMIC PROPERTIES:

Heat of vaporization (liq), kJ/mol	**50.1**
Heat capacity (liq), J/(g.K)	
25°C	**2.10**
Heat of combustion (liq), kJ/mol	**2548**
Enthalpy of formation, (kJ/mol)	**-218.9**

1.3 FLUID PROPERTIES:

Viscosity, mPa.s, 25°C	**4.62**
Surface tension, mN/m (=dyn/cm)	
25°C	**38.2**